ENGINEERING RESEARCH INSTITUTE
DEPARTMENT OF AERONAUTICAL ENGINEERING
UNIVERSITY OF MICHIGAN

DIFFERENTIAL ANALYZER SOLUTION OF THE LINEARIZED F-86D EQUATIONS

By
John W. Peterson
Assistant in Research

Wright-Air Development Center
Department of the Air Force
Contract No. AF 33(616)-2131
E. O. No. R668-421 PO-3a

Interim Technical Report

July, 1954

TABLE OF CONTENTS

	Page
LIST OF FIGURES	iii
TABLE OF SYMBOLS	iv to vi
SUMMARY	1
I. EQUATIONS OF MOTION	1
II. LINEARIZING THE EQUATIONS OF MOTION	3
A. Linearizing the Gravity Forces	4
B. Linearizing the Accelerations	5
C. Linearizing the Engine Forces	6
D. Linearizing the Air Loads	6
E. The Steady State Equations of Motion	8
F. Final Form of the Linearized Equations	8
III. DISCUSSION OF THE LINEARIZED EQUATIONS OF MOTION	9
IV. CORRELATION OF SIMULATOR RESPONSE WITH APPROXIMATE FORMULAS	14
V. CORRELATION WITH FLIGHT TEST DATA	31
VI. MECHANIZATION OF THE EQUATIONS OF MOTION	37

LIST OF FIGURES

Figure		Page
1	Coordinate Axis System	1
2	Simulated Pitching Motion of F-86 D Showing Short Period and Phugoid Response	11
3	Simulated Lateral Motion of F-86 D Showing Short Period Response and Decaying Spiral	12
4	Pitching Motion Response with Simplified Equations	15
5	Lateral Motion Response with Simplified Equations	16
6	Pitching Motion Response with Simplified Equations	17
7	Lateral Motion Response with Simplified Equations	18
8	Pitching Motion Response	19
9	Lateral Motion Response	20
10	Lateral Motion Response Showing Damping of Rolling Motion	21
11	Undamped Natural Period for Pitching Motion (Short Period)	22
12	Damping in Pitch (Short Period)	23
13	Undamped Natural Period for Pitching Motion (Long Period)	26
14	Damping in Pitch (Long Period)	27
15	Undamped Natural Period for Yawing Motion	29
16	Damping of Lateral Motion	30
17	Time Constant of Decaying Spiral	32
18	Time Constant of Uncoupled Rolling Motion	33
19	Flight Test - Simulator Correlation; Short Period Pitching Motion	34
20		36
20	Flight Test - Simulator Correlation; Dynamic Directional Stability Test	36
21	Flight Test - Simulator Correlation; Dynamic Directional Stability Test	38
22	Computer Circuit for Pitching Motion	41
23	Computer Circuit for Lateral Motion	42

TABLE OF SYMBOLS

$\vec{(\ )}$	arrow written over a variable indicates it is a vector.
$(\ ,\ ,\ )$	triad notation indicating the three components of a vector in the body axes coordinate system.
$\bar{(\ )}$	bar written over a variable indicates the perturbation increment of the variable.
$(\ )_o$	subscript zero on a variable means the steady state value of the variable for zero perturbation.
$\dot{(\ )}$	dot over a variable means differentiation with respect to time.
b	airplane wing span, feet.
C	nondimensional airplane coefficient, there are six of these with a single subscript.
C_L, C_D, C_Y	airplane lift, drag, and side-force coefficients.
C_l, C_m, C_n	airplane roll, pitch, and yaw moment coefficients.
C	with two subscripts indicates an airplane stability derivative of which there are fourteen in this analysis.
C_{D_α}	drag curve slope.
C_{L_α}	lift curve slope.
$C_{L_{\dot{\alpha}}}$	lift due to rate of change of angle of attack.
C_{L_q}	lift due to pitching rate.
C_{Y_β}	side force due to yaw.
C_{l_β}	rolling moment due to yaw.
C_{l_p}	damping in roll.
C_{l_r}	rolling moment due to yaw rate.
C_{n_β}	yawing moment due to sideslip (directional stability).
C_{n_p}	yawing moment due to roll.
C_{n_r}	damping in yaw.
C_{m_α}	moment curve slope.
$C_{m_{\dot{\alpha}}}$	moment due to rate of change of angle of attack.

C_{m_q}	damping in pitch.
C	as a subscript to a variable indicates the effect of control surface deflection.
c	as a variable is airplane mean aerodynamic chord, feet.
D	drag force, pounds.
e	as a subscript indicates effect of engine.
$\vec{F} = (X, Y, Z)$	air load force vector, pounds.
g	acceleration of gravity, 32.2 feet per second per second.
$\vec{H}$	airplane angular momentum vector.
h	altitude, feet.
I_{xx}, I_{yy}, I_{zz}	airplane polar moment of inertia relative to the x, y, z body axes, slug-feet squared.
I_{xz}	airplane product of inertia relative to the plane $y = 0$, slug-feet squared.
I	as a subscript means inertial frame of reference.
i	as a subscript means initial value.
$\vec{M} = (L, M, N)$	air load moment vector, pound-feet.
M	mach number.
m	airplane mass slugs.
$\vec{P} = (P_x, P_y, P_z)$	components of engine thrust, pounds.
$\vec{\omega} = (P, Q, R)$ or $(\bar{p}, \bar{q}, \bar{r})$	airplane angular rotation rate vector, radians per second.
q	dynamic pressure $1/2\ \rho\ \lvert\vec{V}\rvert^2$, pounds per square foot.
$\vec{r} = (x, y, z)$	position vector in body axes coordinate system.
S	airplane wing area, square feet.
s	as a subscript indicates stability axes.
t	time, seconds.
$\vec{V} = (U, V, W)$	airplane velocity vector, feet per second.
$(\bar{u}, \bar{v}, \bar{w})$	perturbation of airplane velocity vector, feet per second.
$\vec{F} = (X, Y, Z)$	airplane air load force vector, pounds.

(x, y, z)	position vector in body axes coordinate system.
α	airplane angle of attack.
β	sideslip angle.
$\vec{\gamma} = \gamma_x, \gamma_y, \gamma_z)$	unit gravity vector.
ζ	damping factor.
θ	pitch angle.
λ	root of characteristic equation of linear system.
ρ	mass density of air.
$\vec{\tau} = (\tau_x, \tau_y, \tau_z)$	torque reaction of engine on the airplane.
ϕ	roll angle.

SUMMARY

This report describes an investigation of the dynamic behavior of the F-86D aircraft by means of electronic differential analyzer solutions of the linearized equations of motion. This work is part of an overall study program of the computer section of flight simulators. It is hoped that as a result of this report certain possible simplifications in the configuration of flight computers for fighter aircraft may result.

The equations of motion used in this study are referred to body axes coordinates. These equations are linearized by assuming small perturbations from level flight. In this case linearization results in a system of equations which are uncoupled in such a way that longitudinal pitching motion is independent of lateral motion. The aerodynamic coefficients of the F-86D were substituted into these equations and airplane motion was then simulated on the electronic differential analyzer facility of the Department of Aeronautical Engineering, University of Michigan. The response to a step function input was obtained for four speed-altitude cases. The period and damping of this motion was measured from the traces and compared with approximate formulas.

Correlation with flight test data is also shown. In all cases the agreement was considered to be satisfactory.

I. EQUATIONS OF MOTION

The body axes system of coordinates, shown in Figure 1, are used in this analysis.

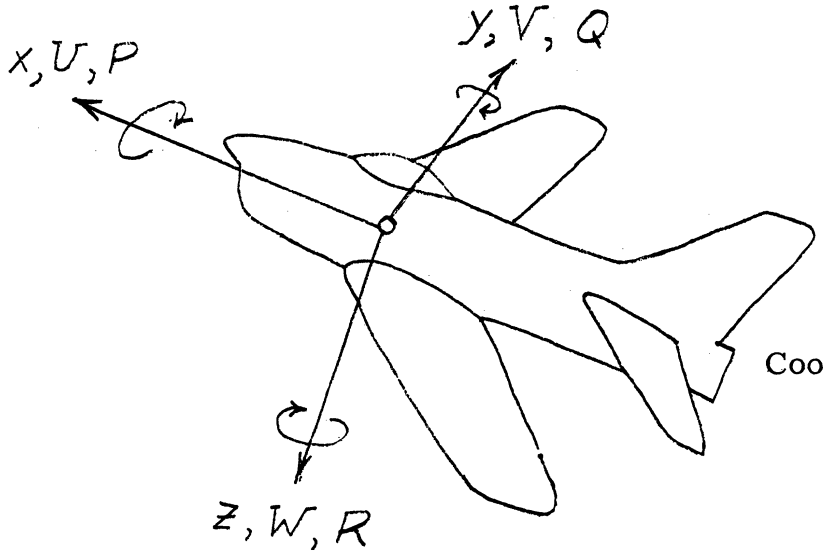


Figure 1

Coordinate Axis System

These axes are orthogonal and fixed with respect to the airplane with the origin at the airplane center of gravity. The airplane velocity with respect to the air is resolved into components along these axes.

$$\vec{V} = (U, V, W)$$

The rotation rate of the airplane which is the same as the rotation of the coordinate frame of reference is

$$\vec{\omega} = (P, Q, R)$$

The equations of motion are obtained from Newton's laws; force equals rate of change of momentum and moment equals rate of change of angular momentum. The forces acting are gravity,

$$mg\vec{\gamma} = mg\,(\gamma_x, \gamma_y, \gamma_z)\,,$$

engine thrust and torque,

$$\vec{P} = (P_x, P_y, P_z)$$

$$\vec{\tau} = (\tau_x, \tau_y, \tau_z)\,,$$

and aerodynamic force and moment due to air loads

$$\vec{F} = (X, Y, Z)$$

$$\vec{M} = (L, M, N)\,.$$

Subscript c indicates loads due to control surface deflection. Therefore

$$\left(\frac{d}{dt}\, m\vec{V}\right)_I = mg\vec{\gamma} + \vec{P} + \vec{F} + \vec{F}_c \qquad (1)$$

$$\left(\frac{d\vec{H}}{dt}\right)_I = \vec{\tau} + \vec{M} + \vec{M}_c \qquad (2)$$

Since the time derivatives in Equations (1) and (2) are relative to inertial coordinates, the component due to rotation of the body axes must be taken into account according to the formula

$$\left[\frac{d(\ )}{dt}\right]_I = \left[(\dot{}) + \vec{\omega} \times (\ )\right] \qquad (3)$$

where the dot means the rate of change relative to body axes coordinates. The angular momentum is

$$\vec{H} = \int \vec{r} \times (\vec{\omega} \times \vec{r})\, dm\,. \qquad (4)$$

where

$$\vec{r} = (x, y, z)$$

The integration is over the whole mass of the airplane. When expanded Equation (4) becomes

$$\vec{H} = (PI_{xx} - QI_{xy} - RI_{xz},\ QI_{yy} - RI_{yz} - PI_{xy},\ RI_{zz} - PI_{xz} - QI_{yz}) \quad (5)$$

where $I_{xx} = \int (y^2 + z^2)\, dm$, $I_{xz} = \int xz\, dm$, etc. The airplane is assumed to be symmetrical with respect to the plane $y = 0$ which leaves I_{xz} the only nonzero product of inertia and (5) becomes

$$\vec{H} = (PI_{xx} - RI_{xz},\ QI_{yy},\ RI_{zz} - PI_{xz}) \quad (6)$$

Hence, by equation (3),

$$\left(\frac{d\vec{H}}{dt}\right)_I = (\dot{P}I_{xx} - \dot{R}I_{xz},\ \dot{Q}I_{yy},\ \dot{R}I_{zz} - \dot{P}I_{xz}) \quad (7)$$

$$+ [QR(I_{zz} - I_{yy}) - PQI_{xz},\ PR(I_{xx} - I_{zz}) + (P^2 - R^2) I_{xz},$$

$$PQ(I_{yy} - I_{xx}) + QRI_{xz}] \ .$$

When equations (1) and (2) are finally expanded according to these formulas the result is

$$\begin{aligned} m(\dot{U} + QW - RV) &= mg\gamma_x + P_x + X + X_c \\ m(\dot{V} + RU - PW) &= mg\gamma_y + P_y + Y + Y_c \\ m(\dot{W} + PV - QU) &= mg\gamma_z + P_z + Z + Z_c \end{aligned} \quad (8)$$

$$\begin{aligned} \dot{P}I_{xx} - \dot{R}I_{xz} + QR(I_{zz} - I_{yy}) - PQI_{xz} &= \tau_x + L + L_c \\ \dot{Q}I_{yy} + PR(I_{xx} - I_{zz}) + (P^2 - R^2) I_{xz} &= \tau_y + M + M_c \\ \dot{R}I_{zz} - \dot{P}I_{xz} + PQ(I_{yy} - I_{xx}) + QRI_{xz} &= \tau_z + N + N_c \end{aligned} \quad (9)$$

II. LINEARIZING THE EQUATIONS OF MOTION

The equations are linearized by considering small perturbations from the steady state of level flight. The steady state angle of attack is

determined by the lift required to balance the weight of the airplane. The angle of attack therefore depends on the steady state speed and altitude and is not assumed to be small. Perturbations from other steady states such as turning motion are possible and would perhaps be considered in more complete studies. It is also possible to compute from linearized equations the motion from an unstable initial state for a short space of time.

The technique of linearizing employed here may be described as follows. The eight quantities U, V, W, P, Q, R, θ, and ϕ are regarded as independent variables and written as the sum of their steady state value plus a perturbation which is denoted by a bar. The absolute value of the steady state velocity vector is denoted by V_o.

$$\begin{aligned} U &= V_o \cos \alpha_o + \bar{u} \\ V &= 0 + \bar{v}, \\ W &= V_o \sin \alpha_o + \bar{w} \\ P &= 0 + \bar{p} \\ Q &= 0 + \bar{q} \\ R &= 0 + \bar{r} \\ \theta &= \alpha_o + \bar{\theta} \\ \phi &= 0 + \bar{\phi} \end{aligned} \tag{10}$$

Each of the terms that appear in the equations of motion are written as explicit functions of these variables, developed in power series of the perturbation variables, and all quadratic and higher powers dropped.

A. Linearizing the Gravity Forces

The orientation of the airplane with respect to vertical is defined by the components of the unit gravity vector $\vec{\gamma}$. Equations which can be used to generate this variable may be derived by applying equation (3) to $\vec{\gamma}$, which is itself a constant vector with respect to inertial axes. Thus

$$\left[\frac{d\vec{\gamma}}{dt}\right]_I = 0 = \dot{\vec{\gamma}} + \vec{\omega} \times \vec{\gamma}. \tag{11}$$

In terms of the body axes components this becomes

$$\begin{aligned} \dot{\gamma}_x &= R\gamma_y - Q\gamma_z \\ \dot{\gamma}_y &= P\gamma_z - R\gamma_x \end{aligned} \tag{12}$$

$$\dot{\gamma}_z = Q\gamma_x - P\gamma_y \ .$$

In this application we want to introduce the pitch and bank angles and linearize. The gravity vector is related to the pitch and bank angles by

$$\vec{\gamma} = (-\sin\theta,\ \cos\theta\sin\phi,\ \cos\theta\cos\phi) \ . \tag{13}$$

In the steady state (13) reduces to

$$\vec{\gamma}_o = (-\sin\alpha_o,\ 0,\ \cos\alpha_o) \tag{14}$$

The perturbation approximation for the gravity vector is therefore

$$\vec{\gamma} \tilde{=} (-\sin\alpha_o - \bar{\theta}\cos\alpha_o,\ \bar{\phi}\cos\alpha_o,\ \cos\alpha_o - \bar{\theta}\sin\alpha_o) \ . \tag{15}$$

From Equations (12) and (13) we have

$$\begin{aligned} \dot{\theta} &= -R\sin\phi + Q\cos\phi \\ \dot{\phi} &= P + \tan\theta\,(Q\sin\phi + R\cos\phi) \ . \end{aligned} \tag{16}$$

The linearized form is

$$\begin{aligned} \dot{\bar{\theta}} &= \bar{q} \\ \dot{\bar{\phi}} &= \bar{p} + \bar{r}\tan\alpha_o \end{aligned} \tag{17}$$

Equations (17) together with the six equations of motion provide a sufficient number of relations among the eight independent variables of the problem.

B. Linearizing the Accelerations

The Coriolis term in the acceleration does not vanish in the linearized case. Substituting (10) in (8) and dropping quadratic perturbation terms,

$$\begin{aligned} \dot{U} + WQ - VR &= \dot{\bar{u}} + V_o\sin\alpha_o\,\bar{q} \\ \dot{V} + UR - WP &= \dot{\bar{v}} + V_o\cos\alpha_o\,\bar{r} - V_o\sin\alpha_o\,\bar{p} \\ \dot{W} + VP - UQ &= \dot{\bar{w}} - V_o\cos\alpha_o\,\bar{q} \end{aligned} \tag{18}$$

In the case of angular acceleration the Coriolis term vanishes. According to Equation (9) these terms are quadratic in the perturbation variables when the steady state is $P = Q = R = 0$. The linearized equations therefore do not take into account precession torques due to rotational airplane motion. Thus,

$$\left.\begin{aligned} \dot{P}I_{xx} - \dot{R}I_{xz} + QR(I_{zz} - I_{yy}) - PQI_{xz} &= \dot{\bar{P}}I_{xx} - \dot{\bar{r}}I_{xz} \\ \dot{Q}I_{yy} + PR(I_{xx} - I_{zz}) + (P^2 - R^2)I_{xz} &= \dot{\bar{q}}I_{yy} \\ \dot{R}I_{zz} - \dot{P}I_{xz} + PQ(I_{yy} - I_{xx}) + QRI_{xz} &= \dot{\bar{r}}I_{zz} - \dot{\bar{p}}I_{xz} \end{aligned}\right\} \quad (19)$$

C. Linearizing the Engine Forces

The engine forces are assumed to be constant in this analysis and therefore the thrust (p) and moments (τ) do not appear in the linearized equations. The torques due to precession of the rotating engine rotor could be taken into account, if necessary, by the equation

$$\vec{\tau} = \vec{\omega} \times (I_e \vec{\omega}_e) . \quad (20)$$

Since the axis of rotation of the engine is the x axis, approximately, (20) becomes

$$\left.\begin{aligned} \tau_x &= 0 \\ \tau_y &= +I_e \omega_e \bar{r} \\ \tau_z &= -I_e \omega_e \bar{q} \end{aligned}\right\} \quad (21)$$

These terms have the effect of coupling the longitudinal and lateral motions.

D. Linearizing the Air Loads

The six components of the air load are

$$\begin{aligned} X &= [-C_D(\alpha)\cos\alpha + C_L(\alpha, \dot{\alpha}, q)\sin\alpha]\, \bar{q}S \\ Y &= +C_Y(\beta)\bar{q}S \\ Z &= -[C_L(\alpha, \dot{\alpha}, q)\cos\alpha + C_D(\alpha)\sin\alpha]\, \bar{q}S \\ L &= [C_\ell(\beta, p_s, r_s)\cos\alpha - C_n(\beta, p_s, r_s)\sin\alpha]\, \bar{q}Sb \\ M &= \alpha C_m(\alpha, \dot{\alpha}, q)\, \bar{q}Sc \\ N &= +[C_n(\beta, p_s, r_s)\cos\alpha + C_\ell(\beta, p_s, r_s)\sin\alpha]\, \bar{q}Sb \end{aligned} \quad (22)$$

The angle of attack factors appear because aerodynamic data is conventionally measured and computed relative to the stability axes rather than the body axes; the transformation involving α must therefore be applied. The parameters on

which these coefficients are assumed to depend are indicated. In some cases it might be desirable to take into account more factors. In Equation (22) the dependences indicated were those for which aerodynamic data was available. The following stability derivatives are therefore involved

$$C_{D_\alpha},\ C_{L_\alpha},\ C_{L_{\dot\alpha}},\ C_{L_q},\ C_{Y_\beta},\ C_{\ell_\beta},\ C_{\ell_p}$$
$$C_{\ell_r},\ C_{n_\beta},\ C_{n_p},\ C_{n_r},\ C_{m_\alpha},\ C_{m_{\dot\alpha}},\ C_{m_q}\ . \tag{23}$$

It is assumed that the p and r stability derivative data used is relative to the stability axis, thus, for example,

$$\bar C_\ell \cong C_{\ell_\beta}\,\bar\beta + C_{\ell_p}\,\bar p_s + C_{\ell_r}\,\bar r_s \tag{24}$$

$$= C_{\ell_\beta}\frac{\bar v}{V_o} + C_{\ell_p}(\bar p\cos\alpha + \bar r\sin\alpha)$$

$$+ C_{\ell_r}(\bar r\cos\alpha - \bar p\sin\alpha)\ .$$

The perturbation in α is derived from

$$\tan\alpha = \frac{W}{U}$$

or

$$\tan(\alpha_o + \bar\alpha) = \frac{V_o\sin\alpha_o + \bar w}{V_o\cos\alpha_o + \bar u} \tag{25}$$

Linearizing each side of equation (25) gives the result

$$\bar\alpha = \frac{\bar w}{V_o}\cos\alpha_o - \frac{\bar u}{V_o}\sin\alpha_o\ . \tag{26}$$

In the case of the forces X and Z which have a nonzero steady state value it is necessary to consider the perturbation in dynamic pressure q,

$$q = q_o + \bar q = q_o\left[1 + 2\left(\frac{\bar u}{V_o}\cos\alpha_o + \frac{\bar w}{V_o}\sin\alpha_o\right)\right]\ . \tag{27}$$

Other useful relations are

$$\left.\begin{aligned}\cos\alpha &\cong \cos\alpha_o - \sin\alpha_o\,\bar\alpha\\ \sin\alpha &\cong \sin\alpha_o + \cos\alpha_o\,\bar\alpha\ .\end{aligned}\right\} \tag{28}$$

E. The Steady State Equations of Motion

The steady state equations are found by equating all perturbations to zero. Equations (8) and (9), together with relations given in (A), (B), (C) and (D) reduce to

$$\left.\begin{aligned}
0 &= -mg\sin\alpha_o + P_x + (-C_{D_o}\cos\alpha_o + C_{L_o}\sin\alpha_o)\,q_o S + X_c \\
0 &= P_y + Y_c \\
0 &= mg\cos\alpha_o + P_z - (C_{L_o}\cos\alpha_o + C_{D_o}\sin\alpha_o)\,q_o S + Z_c \\
0 &= \tau_x + L_c \\
0 &= \tau_y + M_c \\
0 &= \tau_z + N_c
\end{aligned}\right\} \quad (29)$$

The first and third equations were solved for α_o assuming that X_c, Z_c and P_z were all zero and making use of the airplane lift-drag polar. The remaining equations indicate that any asymmetrical engine thrust is compensated by trim.

F. Final Form of the Linearized Equations

When equations (8) and (9) have been subjected to all the linearizing operations outlined above, the following equations result

$$\begin{aligned}
-\dot{\bar{u}} = \frac{q_o S}{mV_o}\Big\{&[(1+\cos^2\alpha_o)\,C_{D_o} - \sin\alpha_o\cos\alpha_o\,(C_{D_\alpha} + C_{L_o}) + \sin^2\alpha_o\,C_{L_\alpha}]\,\bar{u} \\
&+ [-(1+\sin^2\alpha_o)\,C_{L_o} + \sin\alpha_o\cos\alpha_o\,(C_{D_o} - C_{L_\alpha}) + \cos^2\alpha_o\,C_{D_\alpha}]\,\bar{w}\Big\} \\
&- \frac{q_o Sc}{2mV_o}\sin\alpha_o\left[C_{L_q}\bar{q} + C_{L_{\dot\alpha}}\left(\cos\alpha_o\frac{\dot{\bar{w}}}{V_o} - \sin\alpha_o\frac{\dot{\bar{u}}}{V_o}\right)\right] \\
&+ V_o\sin\alpha_o\,\bar{q} + g\cos\alpha_o\,\bar{\theta} \qquad (30) \\
-\dot{\bar{w}} = \frac{q_o S}{mV_o}\Big\{&[(1+\cos^2\alpha_o)\,C_{L_o} + \sin\alpha_o\cos\alpha_o\,(C_{D_o} - C_{L_\alpha}) - \sin^2\alpha_o\,C_{D_\alpha}]\,\bar{u} \\
&+ [C_{D_o} + \cos^2\alpha_o\,C_{L_\alpha} + \sin\alpha_o\cos\alpha_o\,C_{D_\alpha}]\,\bar{w}\Big\} \\
&+ \frac{q_o Sc}{2mV_o}\cos\alpha_o\left[C_{L_q}\bar{q} + C_{L_{\dot\alpha}}\left(\cos\alpha_o\frac{\dot{\bar{w}}}{V_o} - \sin\alpha_o\frac{\dot{\bar{u}}}{V_o}\right)\right]
\end{aligned}$$

$$- V_o \cos \alpha_o \, \bar{q} + g \sin \alpha_o \, \bar{\theta}$$

$$- \dot{\bar{q}} = \frac{q_o S c}{V_o I_{yy}} \left\{ C_{m_\alpha} \sin \alpha_o \, \bar{u} - C_{m_\alpha} \cos \alpha_o \, \bar{w} \right.$$

$$\left. - \frac{c}{2} \left[C_{m_q} \bar{q} + C_{m_{\dot{\alpha}}} \left(\cos \alpha_o \frac{\dot{\bar{w}}}{V_o} - \sin \alpha_o \frac{\dot{\bar{u}}}{V_o} \right) \right] \right\}$$

$$- \dot{\bar{\theta}} = - \bar{q}$$

$$- \dot{\bar{v}} = - \frac{q_o S}{m V_o} C_{y_\beta} \bar{v} - V_o \sin \alpha_o \, \bar{p} + V_o \cos \alpha_o \, \bar{r} - g \cos \alpha_o \, \bar{\phi}$$

$$- \dot{\bar{p}} + \frac{I_{xz}}{I_{xx}} \dot{\bar{r}} = \frac{q_o S b^2}{2 V_o I_{xx}} \left\{ \frac{2}{b} \left(- C_{\ell_\beta} \cos \alpha_o + C_{n_\beta} \sin \alpha_o \right) \bar{v} \right.$$

$$+ \left[- C_{\ell_p} \cos^2 \alpha_o + \left(C_{\ell_r} + C_{n_p} \right) \sin \alpha_o \cos \alpha_o - C_{n_r} \sin^2 \alpha_o \right] \bar{p}$$

$$\left. + \left[- C_{\ell_r} \cos^2 \alpha_o + \left(C_{n_r} - C_{\ell_p} \right) \sin \alpha_o \cos \alpha_o + C_{n_p} \sin^2 \alpha_o \right] \bar{r} \right\}$$

$$- \dot{\bar{r}} + \frac{I_{xz}}{I_{zz}} \dot{\bar{p}} = \frac{q_o S b^2}{2 V_o I_{zz}} \left\{ \frac{2}{b} \left(- C_{n_\beta} \cos \alpha_o - C_{\ell_\beta} \sin \alpha_o \right) \bar{v} \right. \quad (31)$$

$$+ \left[- C_{n_p} \cos^2 \alpha_o + \left(C_{n_r} - C_{\ell_p} \right) \sin \alpha_o \cos \alpha_o + C_{\ell_r} \sin^2 \alpha_o \right] \bar{p}$$

$$\left. + \left[- C_{n_r} \cos^2 \alpha_o - \left(C_{n_p} + C_{\ell_r} \right) \sin \alpha_o \cos \alpha_o - C_{\ell_p} \sin^2 \alpha_o \right] \bar{r} \right\}$$

$$- \dot{\bar{\phi}} = - \bar{p} - \tan \alpha_o \, \bar{r}$$

III. DISCUSSION OF THE LINEARIZED EQUATIONS OF MOTION

The first four equations (30) contain only the variables $\bar{u}$, $\bar{w}$, $\bar{q}$, and $\bar{\theta}$, the second group of four equations (31) involve only the variables $\bar{v}$, $\bar{p}$, $\bar{r}$, and $\bar{\phi}$. Since these equations are linear each system can be solved separately. Motions for which all eight variables are excited may be derived from these solutions by invoking the principle of superposition. Each system

consists of four linear first-order equations in the four variables and is therefore a fourth-order system with four characteristic roots.

The first system, which applies to longitudinal motion, turns out to have a characteristic equation with two pairs of complex conjugate roots for all the cases studied. The response involves a short period oscillatory component and a long period or phugoid component. When the airplane response to a step function input is simulated the short period motion is quickly damped out leaving the phugoid motion which is less rapidly dissipated. The amplitude of oscillation of $\bar{w}$ and $\bar{q}$ is very small for phugoid motion as can be seen in Figure 2. The period and damping of the short period motion can therefore be accurately measured from the $\bar{w}$ or $\bar{q}$ response traces when an initial value has been applied to $\bar{w}$ or $\bar{q}$. The period and damping of the phugoid motion are obtained from the response to an initial value on $\bar{u}$ or $\bar{\theta}$, measuring the damped oscillations which remain when the short period transient has damped out.

The second system of equations for lateral motion also has a short period oscillatory component. However instead of a long period oscillation one finds in this case a pair of exponential functions, one with a short time constant and the other with a long time constant compared with the period of oscillatory motion. The long time constant motion is illustrated in Figure 3 - the short time constant motion in Figure 10. The period and damping of the short period motion can be best measured from the response to an initial value on $\bar{v}$ since this does not excite either exponential component to a great extent. The long time constant can be measured by observing the decay constant of the spiral motion resulting from applying an initial value to $\bar{\phi}$. The short time constant can be measured from the response to an initial value on $\bar{p}$. The response will decay rapidly toward zero with very little residual oscillation.

Equations (30) and (31) can be greatly simplified by setting angle of attack to zero. This may often be a reasonable approximation since the stability derivative data is not very accurately known for a given airplane and the angle of attack is usually not large. If the angle of attack is set to zero only in those terms which involve stability derivatives, equations (30) and (31) reduce to

$$-\dot{\bar{u}} = \frac{\rho_o S}{m V_o}\left[2C_{D_o}\,\bar{u} - (C_{L_o} - C_{D_\alpha})\,\bar{w}\right] + V_o \sin\alpha_o\,\bar{q} + g\cos\alpha_o\,\bar{\theta}$$

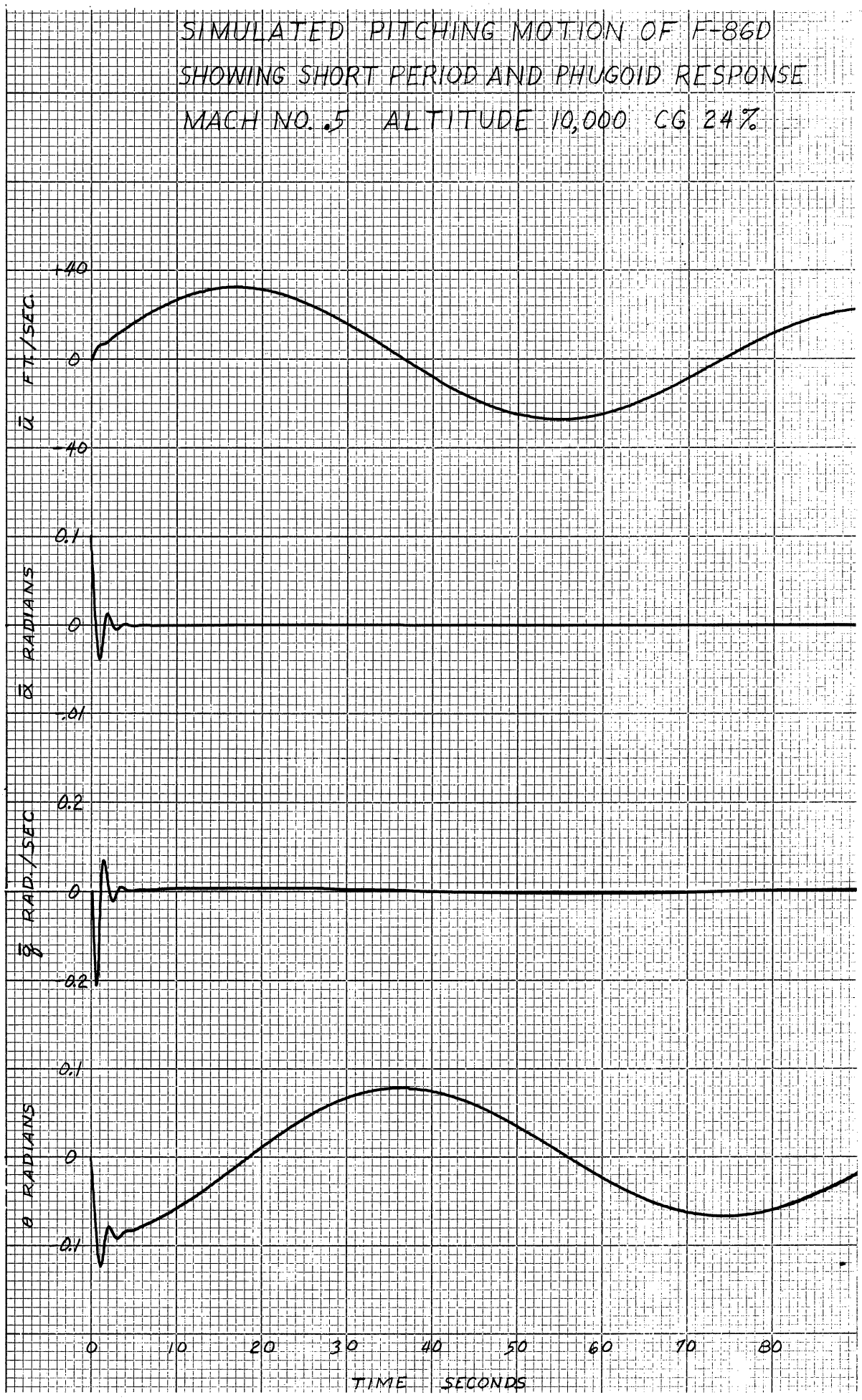

SIMULATED PITCHING MOTION OF F-86D
SHOWING SHORT PERIOD AND PHUGOID RESPONSE
MACH NO. .5 ALTITUDE 10,000 CG 24%
+40
0
-40
u FT./SEC.
0.1
0
-.01
α RADIANS
0.2
0
-.02
q RAD./SEC.
0.1
0
-0.1
θ RADIANS
0
10
20
30
40
50
60
70
80
TIME SECONDS

Figure 2

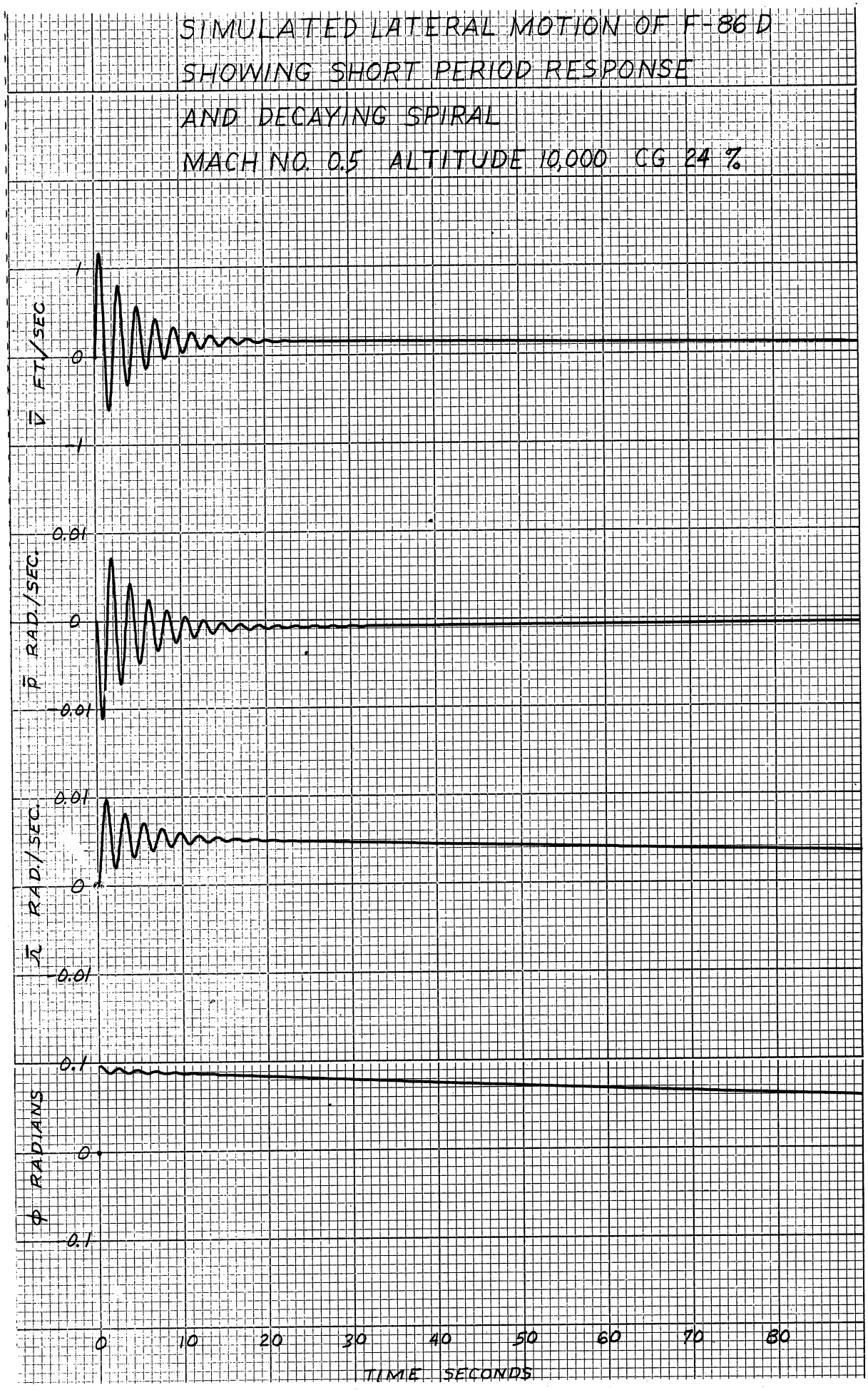

SIMULATED LATERAL MOTION OF F-86 D
SHOWING SHORT PERIOD RESPONSE
AND DECAYING SPIRAL
MACH NO. 0.5 ALTITUDE 10,000 CG 24 %
$\bar{v}$ FT/SEC
1
0
-1
$\bar{p}$ RAD./SEC.
0.01
0
-0.01
$\bar{r}$ RAD./SEC.
0.01
0
-0.01
ϕ RADIANS
0.1
0
-0.1
0
10
20
30
40
50
60
70
80
TIME SECONDS

Figure 3

$$-\dot{\bar{w}} = \frac{q_o S}{mV_o}\left[2C_{L_o}\bar{u} + (C_{D_o} + C_{L_\alpha})\bar{w} + \frac{c}{2}\left(C_{L_q}\bar{q} + C_{L_{\dot{\alpha}}}\frac{\dot{\bar{w}}}{V_o}\right)\right]$$

$$- V_o \cos\alpha_o \bar{q} + g \sin\alpha_o \bar{\theta} \qquad (32)$$

$$-\dot{\bar{q}} = \frac{q_o Sc}{V_o I_{yy}}\left[-C_{m_\alpha}\bar{w} - \frac{c}{2}\left(C_{m_q}\bar{q} + C_{m_{\dot{\alpha}}}\frac{\dot{\bar{w}}}{V_o}\right)\right]$$

$$-\dot{\bar{\theta}} = -\bar{q}$$

$$-\dot{\bar{v}} = -\frac{q_o Sc}{mV_o} C_{y_\beta}\bar{v} - V_o \sin\alpha_o \bar{p} + V_o \cos\alpha_o \bar{r} - g\cos\alpha_o \bar{\phi}$$

$$-\dot{\bar{p}} + \frac{I_{xz}}{I_{xx}}\dot{\bar{r}} = \frac{q_o Sb^2}{2V_o I_{xx}}\left[-\frac{2}{b}C_{\ell_\beta}\bar{v} - C_{\ell_p}\bar{p} - C_{\ell_r}\bar{r}\right] \qquad (33)$$

$$-\dot{\bar{r}} + \frac{I_{xz}}{I_{zz}}\dot{\bar{p}} = \frac{q_o Sb^2}{2V_o I_{zz}}\left[-\frac{2}{b}C_{n_\beta}\bar{v} - C_{n_p}\bar{p} - C_{n_r}\bar{r}\right]$$

$$-\dot{\bar{\phi}} = -\bar{p} - \tan\alpha_o \bar{r} \ .$$

A further simplification would be to set the angle of attack to zero in the remaining terms which are Coriolis acceleration terms and gravity forces. The resulting systems of equations are

$$-\dot{\bar{u}} = \frac{q_o S}{mV_o}\left[2C_{D_o}\bar{u} - (C_{L_o} - C_{D_\alpha})\bar{w}\right] + g\bar{\theta}$$

$$-\dot{\bar{w}} = \frac{q_o S}{mV_o}\left[2C_{L_o}\bar{u} + (C_{D_o} + C_{L_\alpha})\bar{w} + \frac{c}{2}\left(C_{L_q}\bar{q} + C_{L_{\dot{\alpha}}}\frac{\dot{\bar{w}}}{V_o}\right)\right] - V_o\bar{q}$$

$$-\dot{\bar{q}} = \frac{q_o Sc}{V_o I_{yy}}\left[-C_{m_\alpha}\bar{w} - \frac{c}{2}\left(C_{m_q}\bar{q} + C_{m_{\dot{\alpha}}}\frac{\dot{\bar{w}}}{V_o}\right)\right] \qquad (34)$$

$$-\dot{\bar{\theta}} = -\bar{q}$$

$$-\dot{\bar{v}} = -\frac{q_o Sc}{mV_o} C_{y_\beta}\bar{v} + V_o\bar{r} - g\bar{\phi}$$

$$-\dot{\bar{p}} + \frac{I_{xz}}{I_{xx}}\dot{\bar{r}} = \frac{q_o Sb^2}{2V_o I_{xx}}\left[-\frac{2}{b}C_{\ell_\beta}\bar{v} - C_{\ell_p}\bar{p} - C_{\ell_r}\bar{r}\right]$$

$$-\dot{\bar{r}} + \frac{I_{xz}}{I_{zz}}\dot{\bar{p}} = \frac{q_o S b^2}{2V_o I_{zz}}\left[-\frac{2}{b}C_{n_\beta}\bar{v} - C_{n_p}\bar{p} - C_{n_r}\bar{r}\right] \qquad (35)$$

$$-\bar{\phi} = -\bar{p}\,.$$

The order of the systems of equations have not been reduced by these simplifications. The change in the response due to these approximations is shown for a moderate and a high angle of attack in Figures 4, 5, 6, and 7. It is seen that in the case of lateral motion the Coriolis terms cannot be approximated successfully, especially at high angles of attack. The other approximations all agree quite well with the exact linearized equations. Such approximations do not gain much in the present application since the coefficients are evaluated before bringing the problem to the computer. However a simulator which automatically generates these coefficients as functions of speed and altitude would be simpler in design if these approximations were made.

IV. CORRELATION OF SIMULATOR RESPONSE WITH APPROXIMATE FORMULAS

Measurements of the simulator response were made for four speed altitude cases. Eight parameters are measured, corresponding to the four characteristic roots of the pitching motion and four also for lateral motion. This data was taken from Brush recorder tapes in the case of the short period oscillating motions and damping in roll. Figures 8, 9, and 10 are examples of this data. This recording equipment has adequate frequency response for rapidly changing variables. Phugoid motion and spiral decay data were read directly from servo dials since these motions change very slowly. Approximate formulas are derived in this section for all cases. Figures 11 through 18 show these formulas plotted as curves and also points obtained from the more exact simulator response traces.

The approximate formula for short period pitching motion may be derived from Equations (34) by assuming the change in the forward component of velocity, $\bar{u}$, is small. The second and third equation then uncouple from the first and fourth, and equations (33) degenerate to the second-order system.

$$-\dot{\bar{w}} = \frac{q_o S}{mV_o}\left[(C_{D_o} + C_{L_\alpha})\bar{w} + \frac{C}{2}\left(C_{L_q}\bar{q} + C_{L_{\dot{\alpha}}}\frac{\dot{\bar{w}}}{V_o}\right)\right] - V_o\bar{q}$$

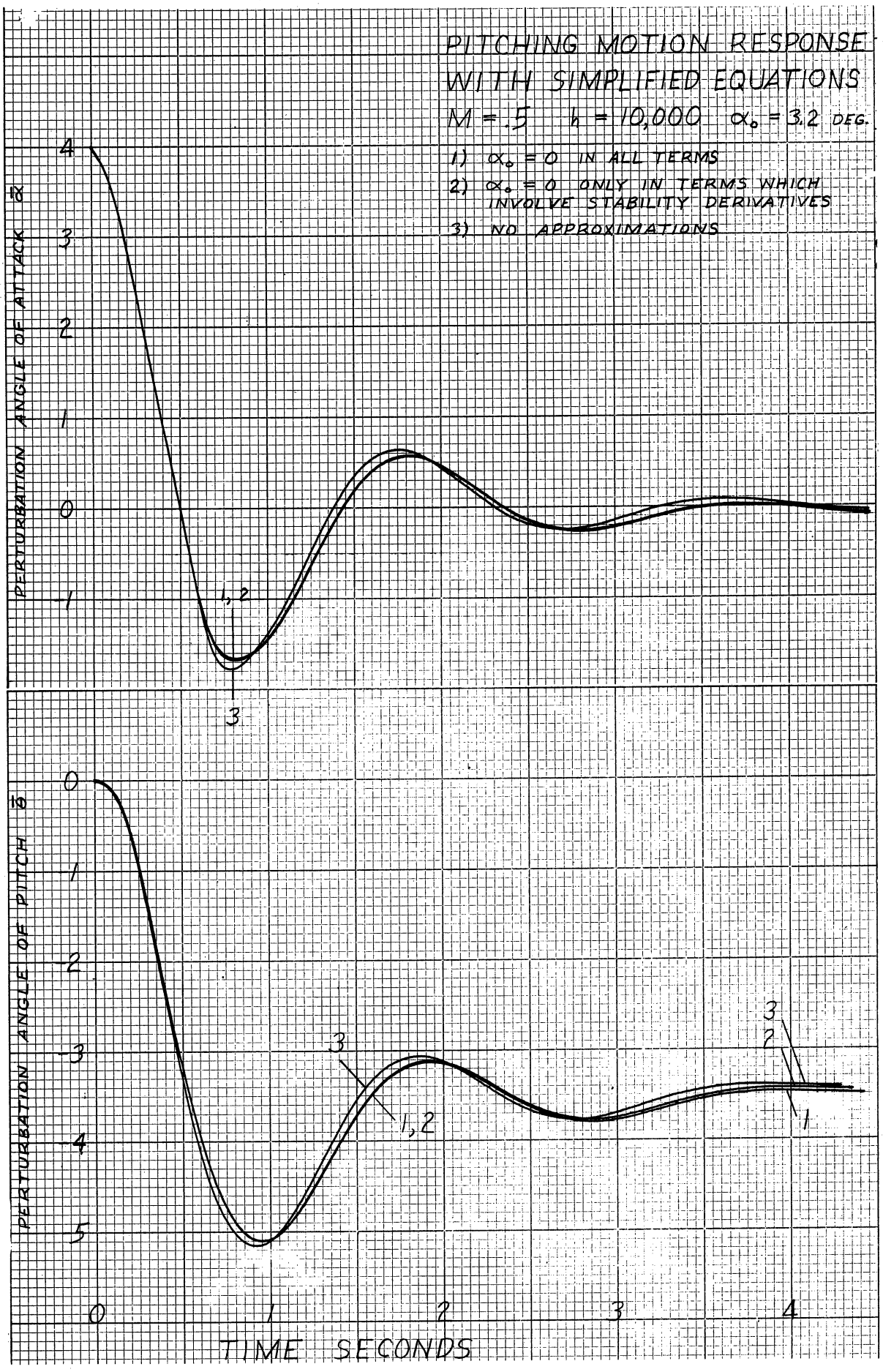

PITCHING MOTION RESPONSE
WITH SIMPLIFIED EQUATIONS
M = .5 h = 10,000 α_0 = 3.2 DEG.
1) $\alpha_0 = 0$ IN ALL TERMS
2) $\alpha_0 = 0$ ONLY IN TERMS WHICH INVOLVE STABILITY DERIVATIVES
3) NO APPROXIMATIONS
PERTURBATION ANGLE OF ATTACK α
PERTURBATION ANGLE OF PITCH θ
TIME SECONDS
1, 2
3
0
1
2
3
4
5

Figure 4

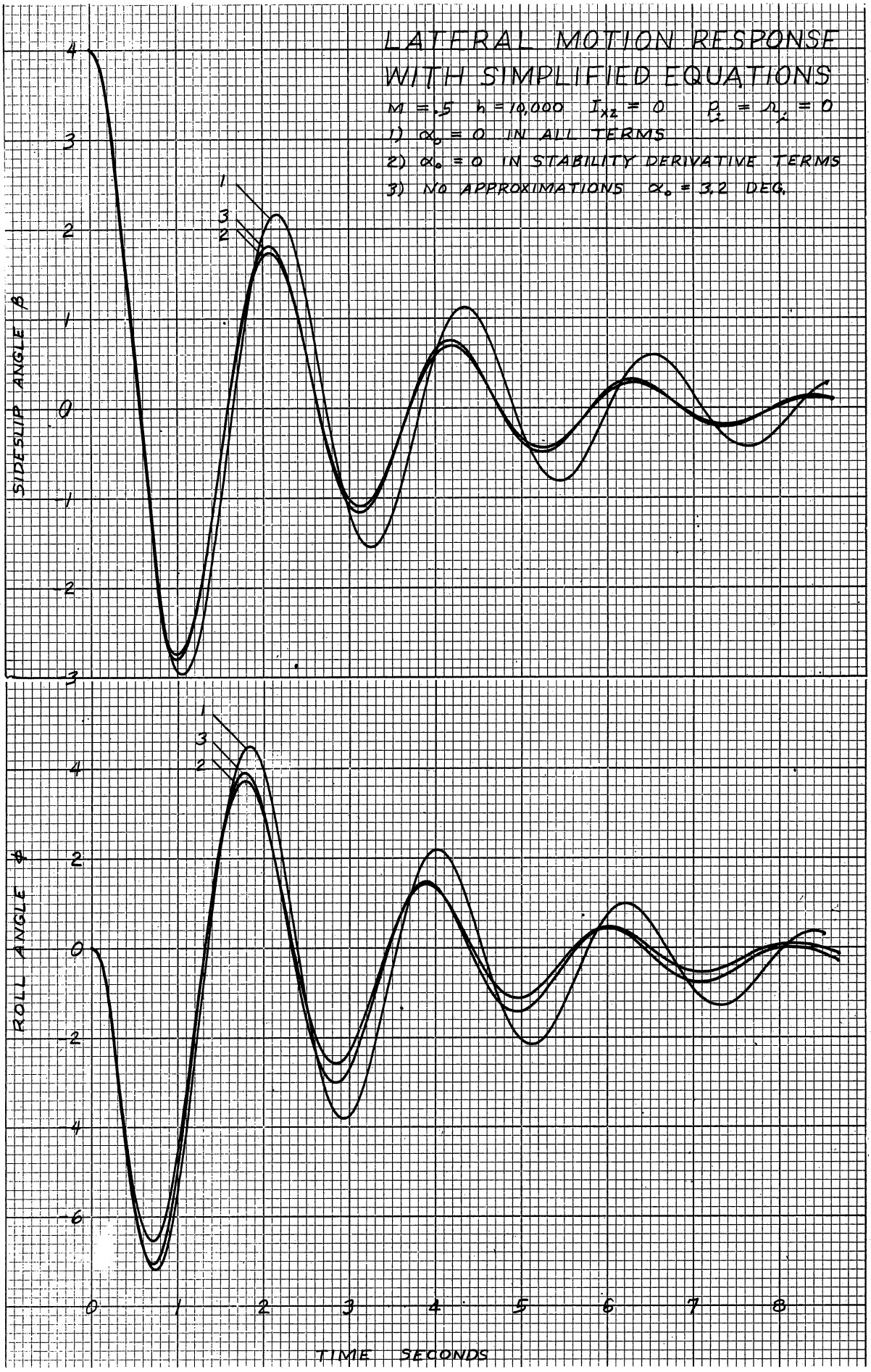

LATERAL MOTION RESPONSE
WITH SIMPLIFIED EQUATIONS
M = .5 h = 10,000 I_{xz} = 0 p_z = n_z = 0
1) α_o = 0 IN ALL TERMS
2) α_o = 0 IN STABILITY DERIVATIVE TERMS
3) NO APPROXIMATIONS α_o = 3.2 DEG.
SIDESLIP ANGLE β
ROLL ANGLE φ
TIME SECONDS
1
2
3

Figure 5

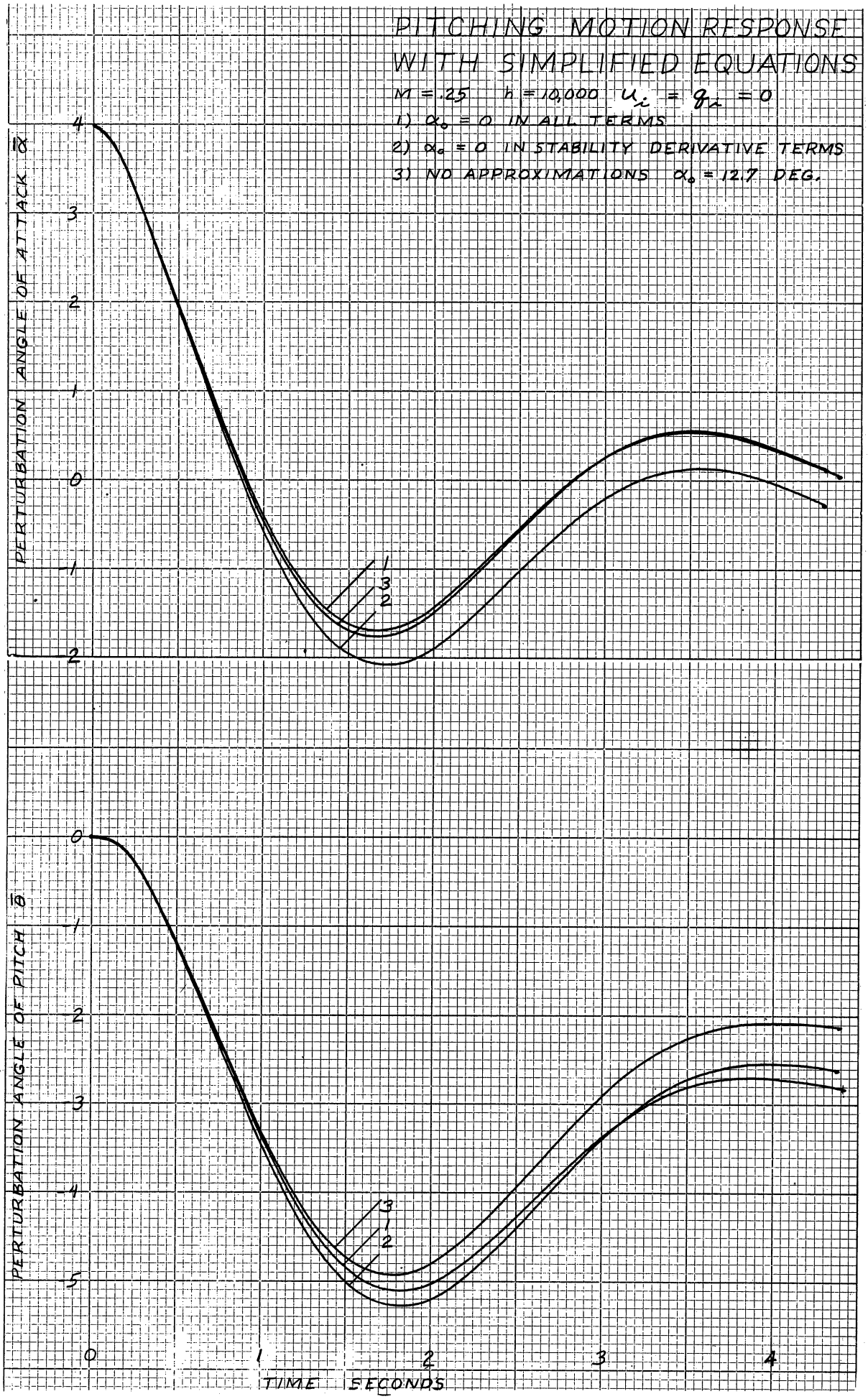

PITCHING MOTION RESPONSE
WITH SIMPLIFIED EQUATIONS
M = .25 h = 10,000 $u_i = q_a = 0$
1) $\alpha_0 = 0$ IN ALL TERMS
2) $\alpha_0 = 0$ IN STABILITY DERIVATIVE TERMS
3) NO APPROXIMATIONS $\alpha_0 = 12.7$ DEG.
PERTURBATION ANGLE OF ATTACK $\bar{\alpha}$
PERTURBATION ANGLE OF PITCH $\bar{\theta}$
TIME SECONDS
4
3
2
1
0
-1
-2
-3
-4
-5
0
1
2
3
4
1
3
2
3
1
2

Figure 6

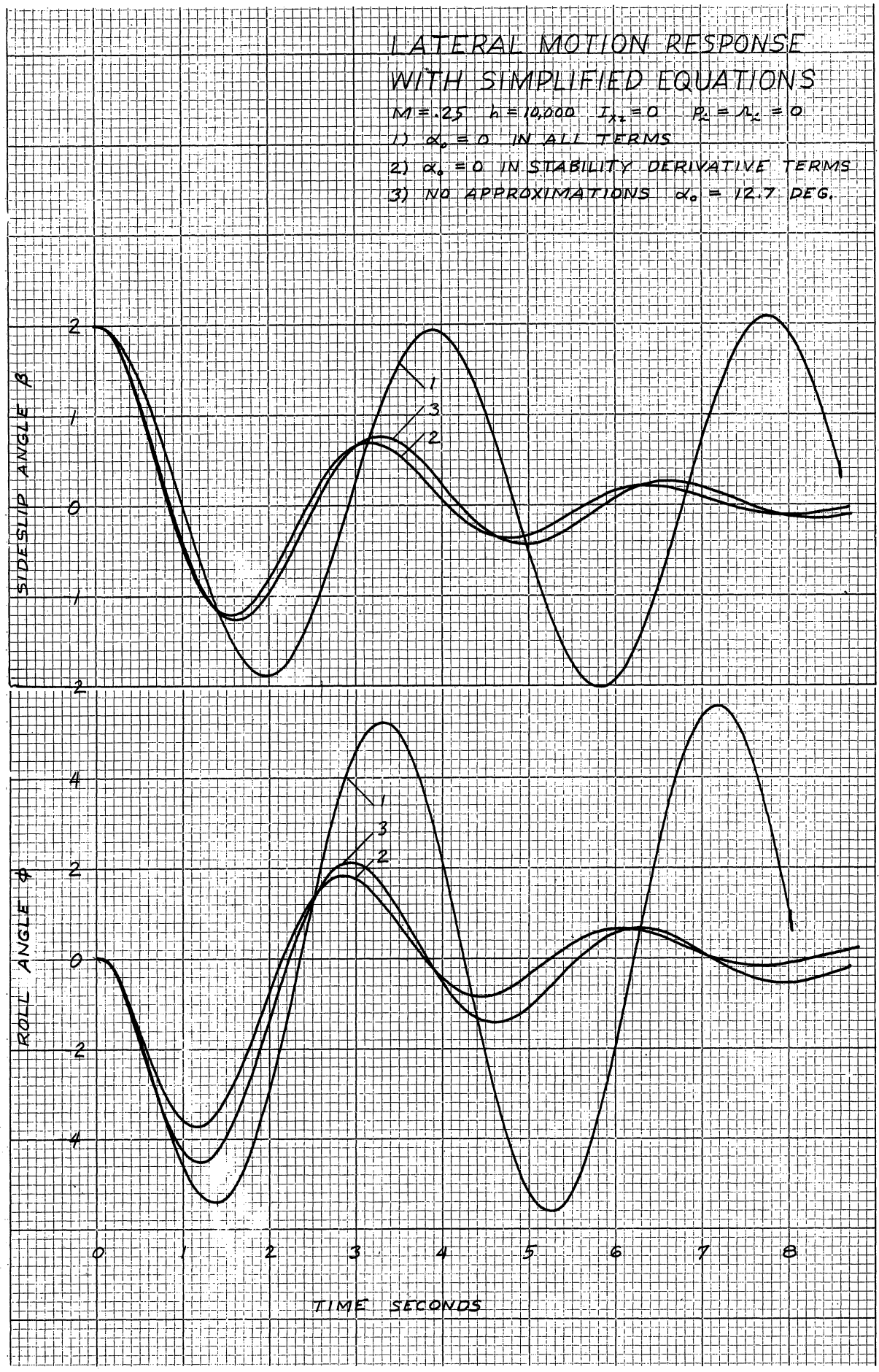

LATERAL MOTION RESPONSE
WITH SIMPLIFIED EQUATIONS
M = .25 h = 10,000 $I_{xz} = 0$ $p_{\dot{\beta}} = r_{\dot{\beta}} = 0$
1) $\alpha_0 = 0$ IN ALL TERMS
2) $\alpha_0 = 0$ IN STABILITY DERIVATIVE TERMS
3) NO APPROXIMATIONS $\alpha_0 = 12.7$ DEG.
SIDESLIP ANGLE β
ROLL ANGLE φ
TIME SECONDS
1
2
3

Figure 7

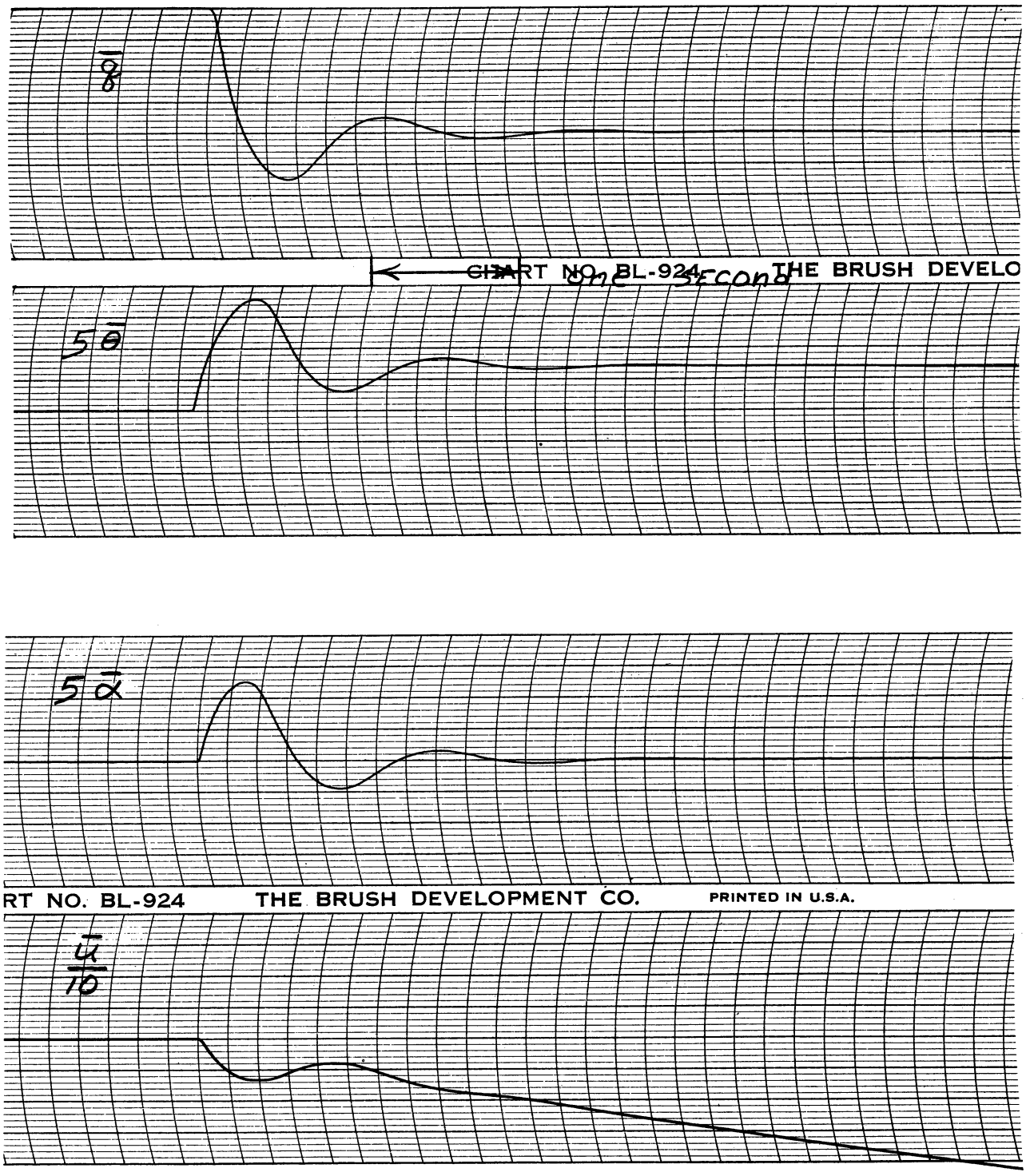


Figure 8. Pitching Motion Response

Mach Number 0.7
Altitude 10,000 feet
Damping factor 0.32
Undamped natural period 1.28 seconds

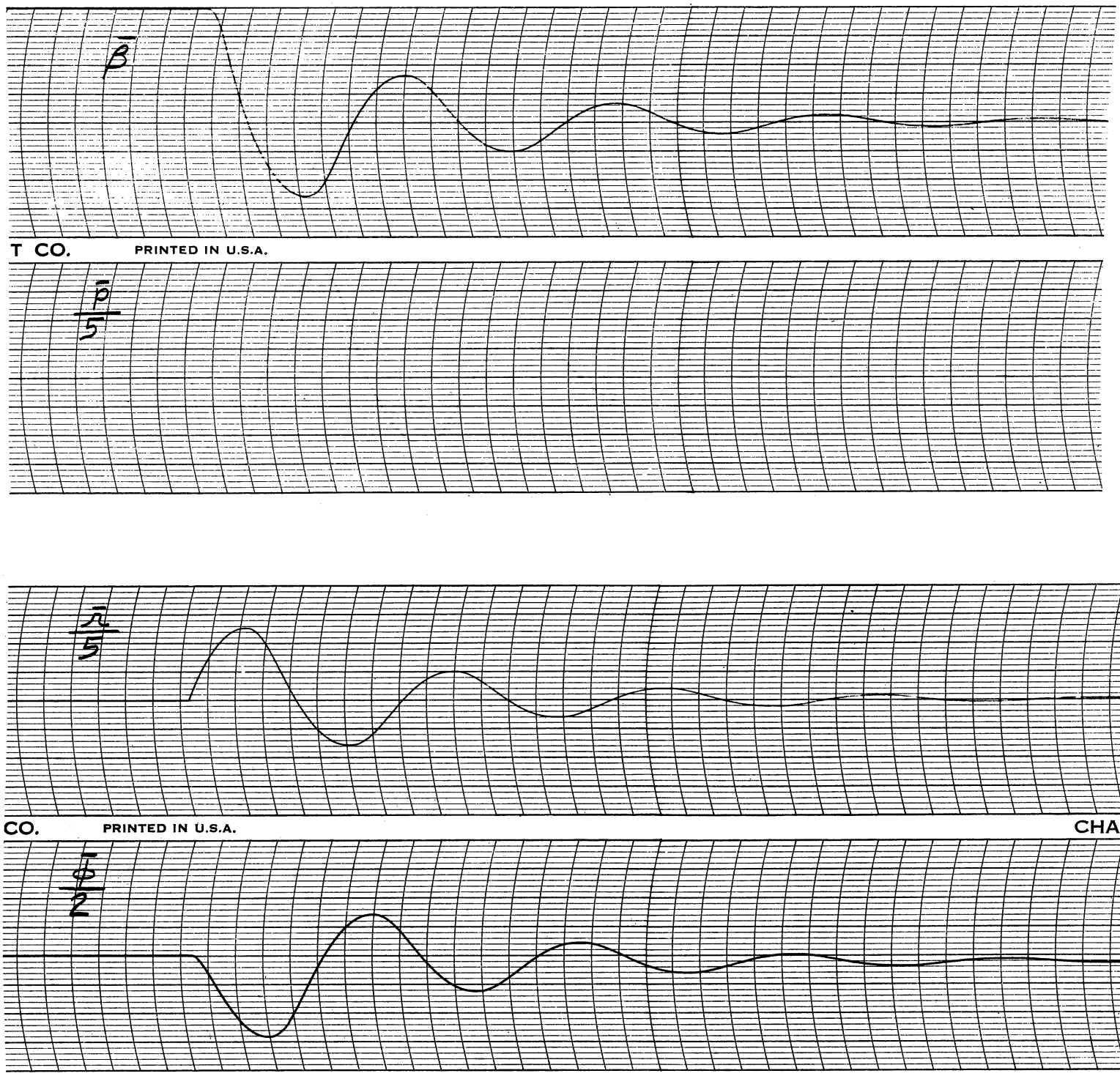


Figure 9. Lateral Motion Response

Mach Number 0.7
Altitude 10,000 feet
Damping factor
Undamped natural period

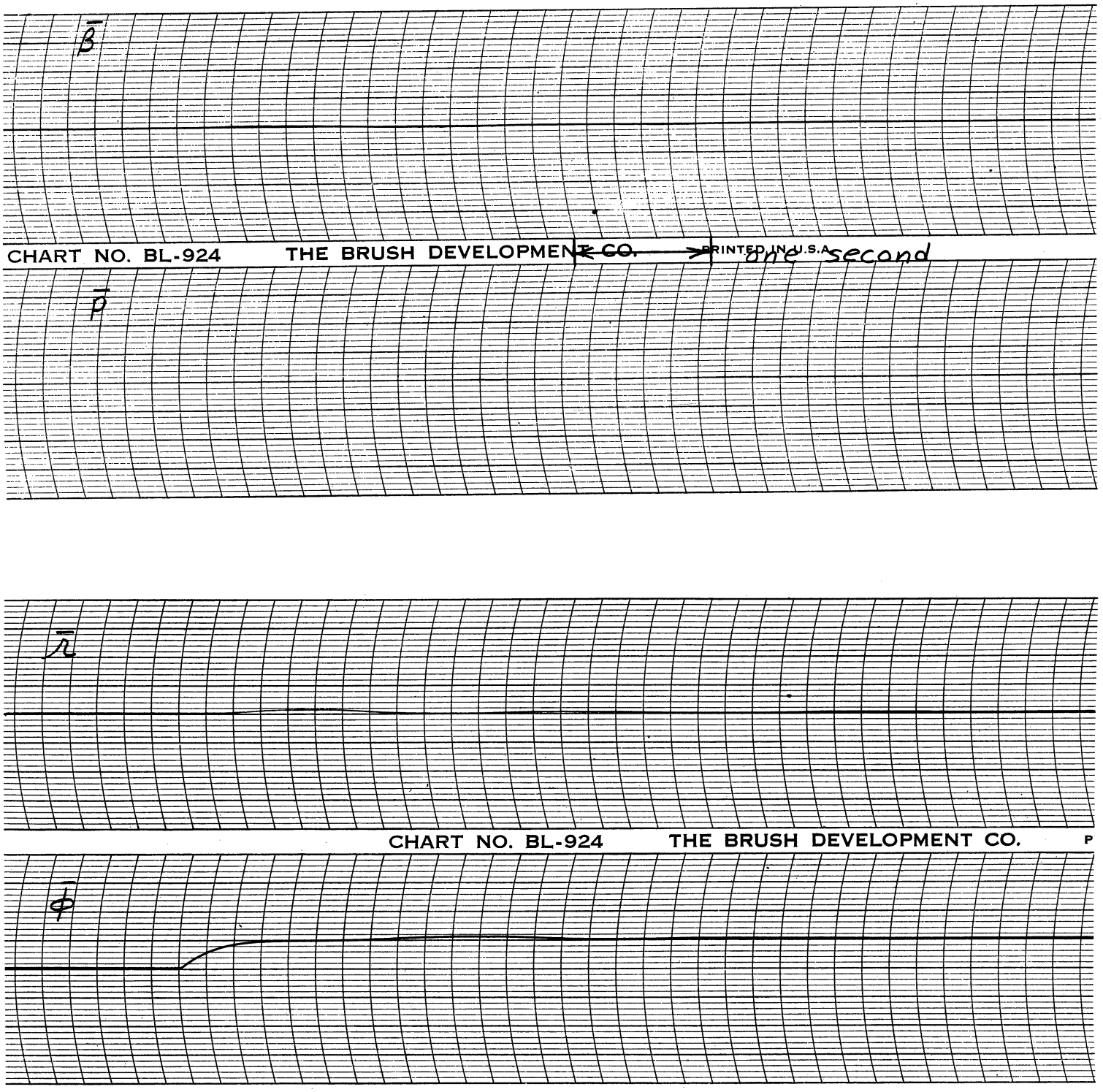


Figure 10. Lateral Motion Response Showing Damping of Rolling Motion

Mach Number 0.8
Altitude 30,000 feet

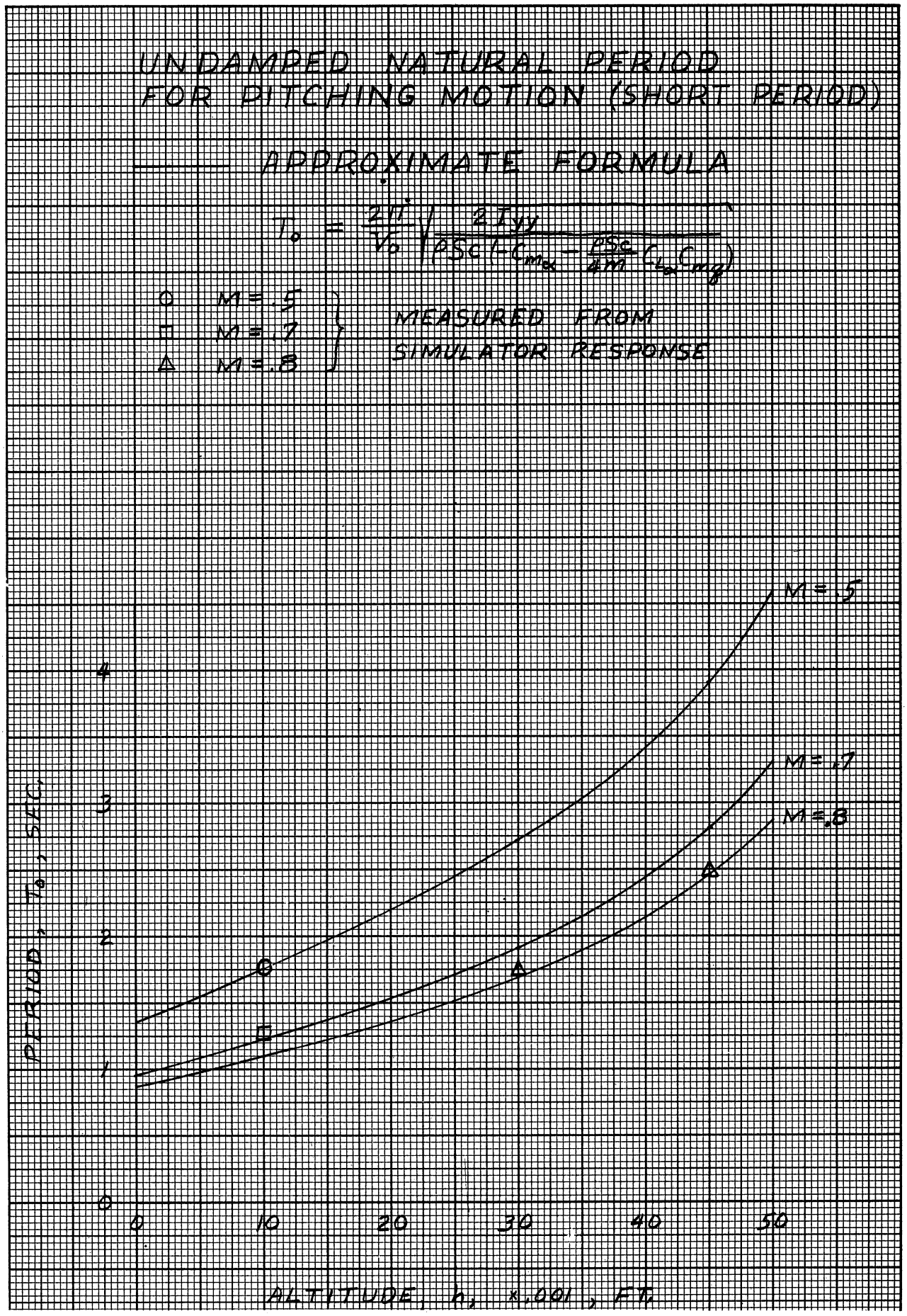

UNDAMPED NATURAL PERIOD
FOR PITCHING MOTION (SHORT PERIOD)
APPROXIMATE FORMULA
$T_0 = \frac{2\pi}{V_0}\sqrt{\frac{2I_{yy}}{\rho S c\left(-C_{m_{\dot\alpha}} - \frac{\rho S c^2}{4m} C_{L_\alpha} C_{m_q}\right)}}$
○ M = .5
□ M = .7
△ M = .8
MEASURED FROM SIMULATOR RESPONSE
M = .5
M = .7
M = .8
PERIOD, T_0, SECONDS
0
1
2
3
4
0
10
20
30
40
50
ALTITUDE, h_p x.001, FT.

Figure 11

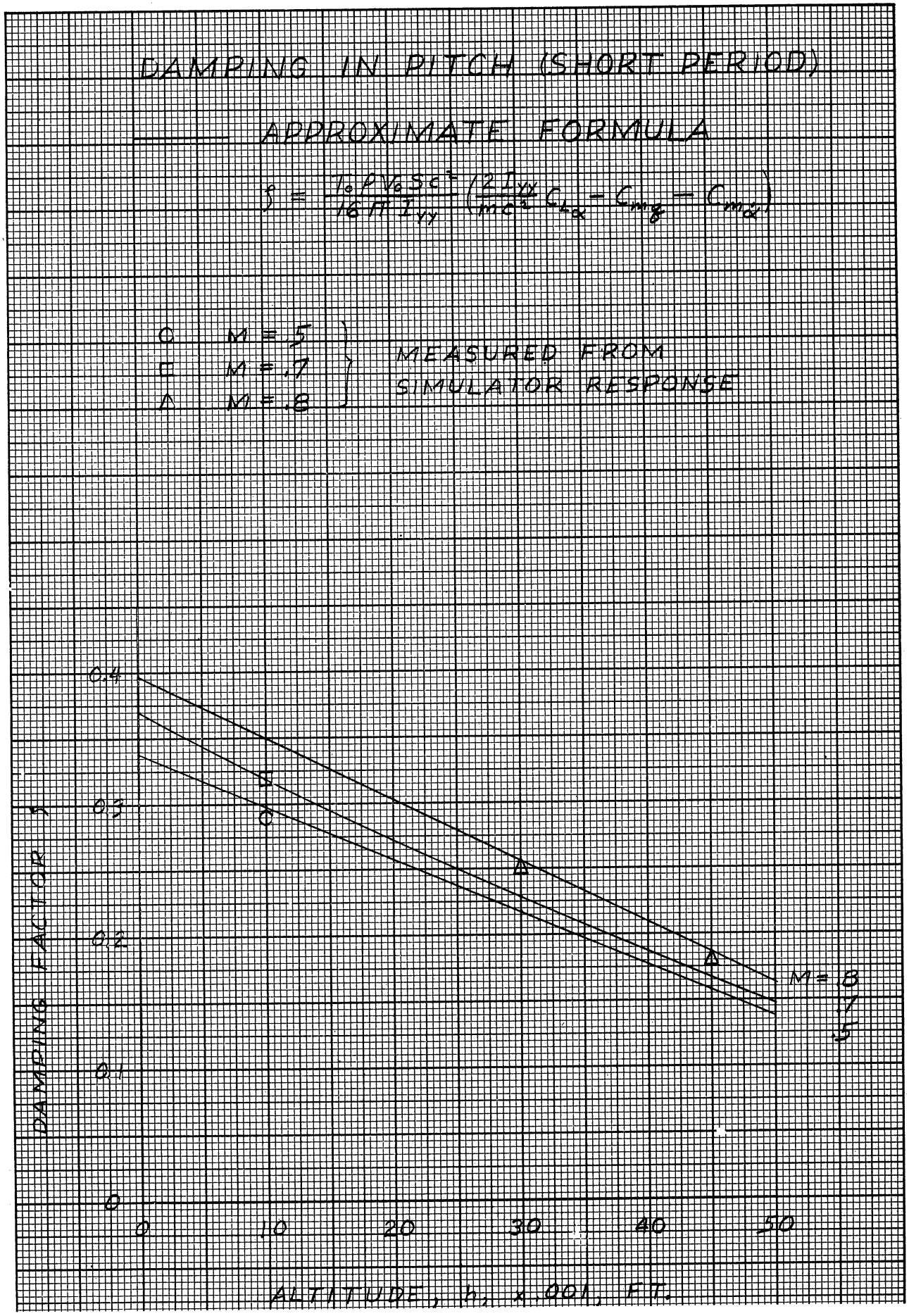

DAMPING IN PITCH (SHORT PERIOD)
APPROXIMATE FORMULA
$\zeta = \frac{T_0 \rho V_0 S c^2}{16 I_{yy}} \left(\frac{2 I_{yy}}{m c^2} C_{L_\alpha} - C_{m_{\dot{\alpha}}} - C_{m_q} \right)$
○ M = .5
□ M = .7
△ M = .8
MEASURED FROM SIMULATOR RESPONSE
DAMPING FACTOR, ζ
0.4
0.3
0.2
0.1
0
0
10
20
30
40
50
M = .8
.7
.5
ALTITUDE, h_p x 1001 FT.

Figure 12

$$-\dot{\bar{q}} = \frac{q_o Sc}{V_o I_{yy}} \left[- C_{m_\alpha} \bar{w} - \frac{c}{2} \left(C_{m_q} \bar{q} + C_{m_{\dot\alpha}} \frac{\dot{\bar{w}}}{V_o} \right) \right] . \qquad (36)$$

Since C_{D_o}, $C_{L_{\dot\alpha}}$, and C_{L_q} are small and have a negligible effect they are also omitted. The characteristic equation of the system (36) is

$$\begin{vmatrix} \frac{q_o S}{mV_o} C_{L_\alpha} + \lambda & - V_o \\ - C_{m_\alpha} - \frac{c}{2} C_{m_{\dot\alpha}} \frac{\lambda}{V_o} & - \frac{c}{2} C_{m_q} + \frac{V_o I_{yy}}{q_o SC} \lambda \end{vmatrix} = 0 \qquad (37)$$

The roots are complex. The undamped natural period and the damping corresponding to these roots are

$$T_o = \frac{2\pi}{V_o} \sqrt{\frac{2I_{yy}}{\rho Sc \left(- C_{m_\alpha} - \frac{\rho Sc}{4m} C_{L_\alpha} C_{m_q} \right)}} \qquad (38)$$

$$\zeta = \frac{T_o \rho V_o Sc^2}{16\pi I_{yy}} \left(\frac{2I_{yy}}{mc^2} C_{L_\alpha} - C_{m_q} - C_{m_{\dot\alpha}} \right).$$

The damping factor can be measured from the amplitude of the decaying oscillations. In this case the damping factor cannot be found by comparing the amplitude of the overshoot with the initial displacement since the initial value does not correspond to a maximum excursion. Figures 11 and 12 show this data.

The approximate formula for phugoid motion can be derived from (34) by assuming that the angle of attack, which is proportional to $\bar{w}$, does not change appreciably. Since $mg = C_{L_o} q_o S$ these equations reduce to

$$-\dot{\bar{u}} = 2 \frac{g}{V_o} \frac{C_{D_o}}{C_{L_o}} \bar{u} + g\theta$$

$$0 = 2 \frac{g}{V_o} \bar{u} - V_o \bar{q} \qquad (39)$$

$$-\dot{\bar{\theta}} = -\bar{q}$$

The second-order system (39) has period and damping given by the formulas

$$T_o = \sqrt{2}\,\pi\, V_o/g$$
$$\zeta = C_{D_o}/\sqrt{2}\, C_{L_o} \tag{40}$$

The period is not a function of any airplane parameter. Figures (13) and (14) exhibit this data. The satisfactory simulator performance is significant since computer circuits can often be designed to function better over a restricted range or to work best in one range at the expense of another range of variables. In this case, however, the same computer circuit was used for these two greatly different types of motion.

An approximate formula for the oscillatory lateral motion which is very similar to the formula for pitching motion can be obtained in certain cases. In equations (35) with $I_{xz} = 0$, if $\bar{\phi}$ is dropped from the first equation and $\bar{p}$ from the third equation, a second-order system results. One would expect this approximation would be most satisfactory at high speeds and low altitudes since then the inequalities $g << V_o$ and $c_{np} << c_{n_r}$ are strongest. This assumption does not mean the airplane does not roll much (as a matter of fact it rolls about twice as much as it yaws) but rather that the rolling does not affect the rest of the system very much due to the small coupling term. The second order system is

$$-\dot{\bar{v}} = -\frac{q_o Sc}{mV_o} C_{Y_\beta}\, \bar{v} + V_o\, \bar{r}$$
$$-\dot{\bar{r}} = -\frac{q_o Sb^2}{2V_o I_{zz}} \left(\frac{2}{b} C_{n_\beta}\, \bar{v} + C_{n_r}\, \bar{r}\right). \tag{41}$$

The period and damping for this system is

$$T_o = \frac{2\pi}{V_o}\sqrt{\frac{2I_{zz}}{\rho Sb\left(C_{n_\beta} + \frac{\rho Sb}{4m} C_{Y_\beta} C_{n_r}\right)}}$$
$$\zeta = \frac{T_o \rho V_o Sb^2}{16\pi I_{zz}} \left(-\frac{2I_{zz}}{mb^2} C_{Y_\beta} - C_{n_r}\right). \tag{42}$$

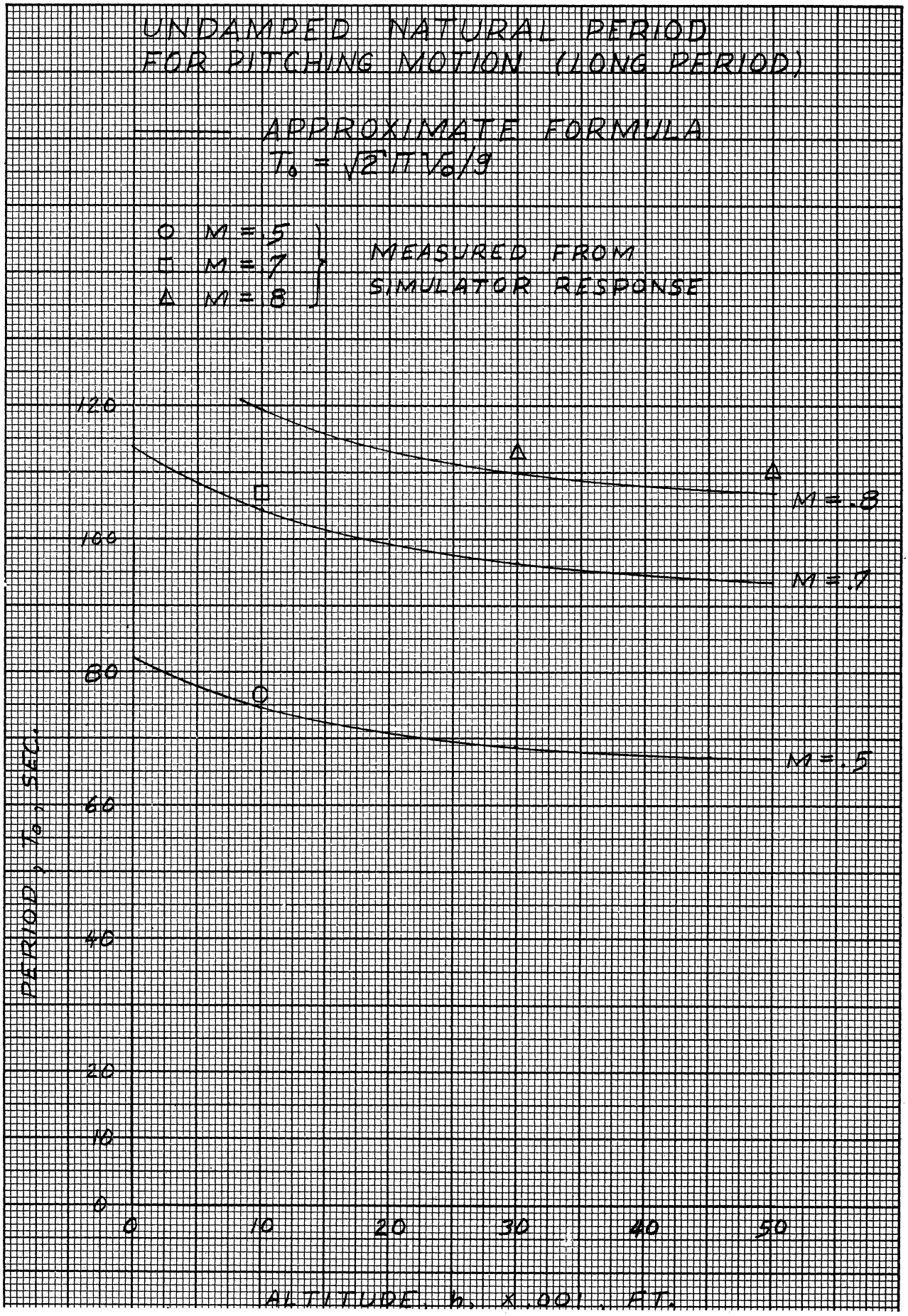

UNDAMPED NATURAL PERIOD
FOR PITCHING MOTION (LONG PERIOD).
APPROXIMATE FORMULA
$T_0 = \sqrt{2}\pi V_0/g$
○ M = .5
□ M = .7
△ M = .8
MEASURED FROM
SIMULATOR RESPONSE
120
100
80
60
40
20
10
0
PERIOD, T_0, SEC.
0
10
20
30
40
50
ALTITUDE, h, X.001, FT.
M = .8
M = .7
M = .5

Figure 13

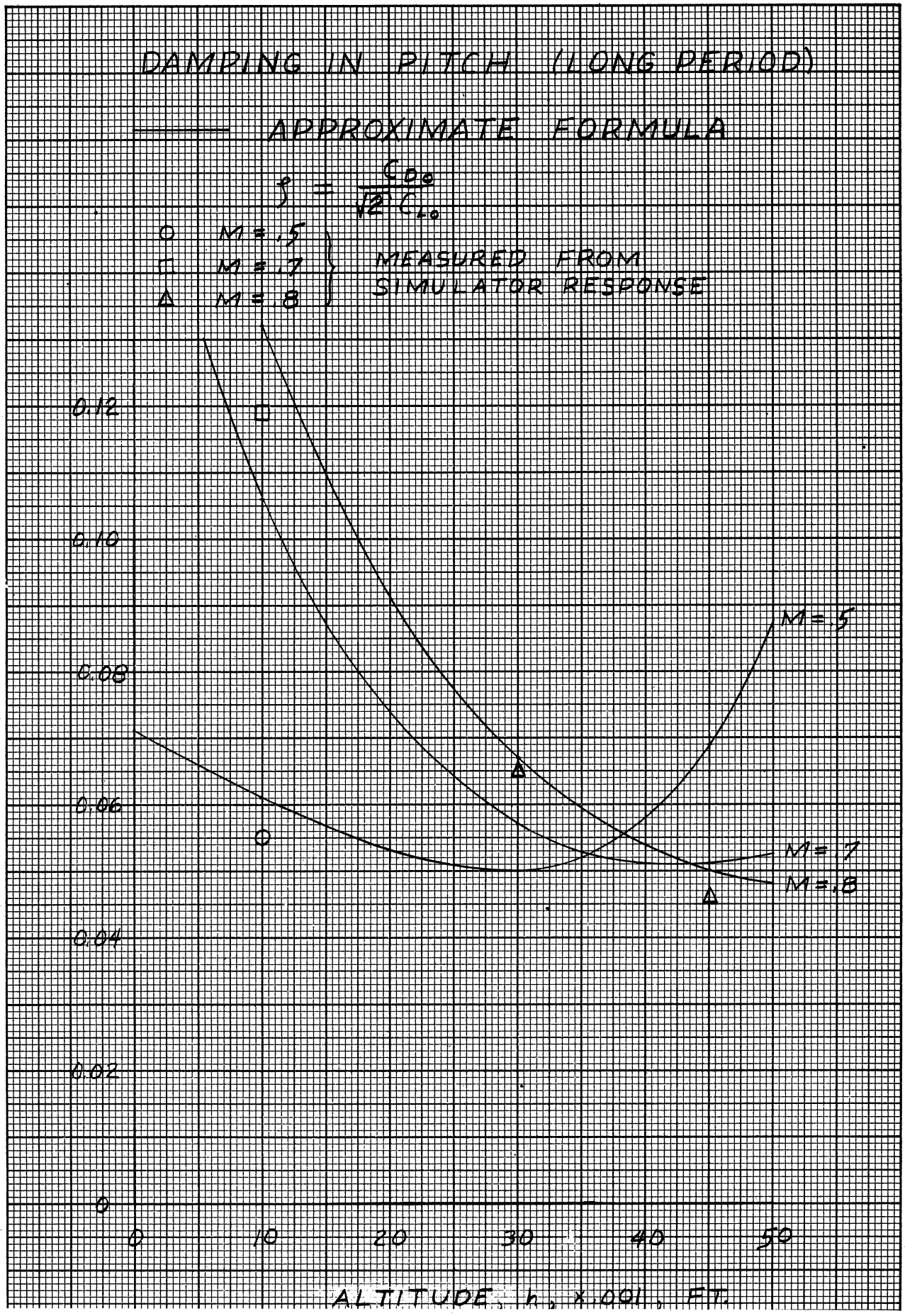

DAMPING IN PITCH (LONG PERIOD)
APPROXIMATE FORMULA
$\zeta = \frac{C_{D_0}}{\sqrt{2}\, C_{L_0}}$
○ M = .5
□ M = .7
△ M = .8
MEASURED FROM SIMULATOR RESPONSE
0.12
0.10
0.08
0.06
0.04
0.02
0
M = .5
M = .7
M = .8
0
10
20
30
40
50
ALTITUDE, h, x.001, FT.

Figure 14

These formulas are compared with the simulator responses in Figures 15 and 16. The periods check very well and also the damping except at the higher altitudes where the assumptions made are most questionable.

When operating the simulator it was found that spiral motion was a very slowly changing phenomenon. Therefore it seemed reasonable to approximate this by setting all the accelerations to zero. Equations (35) then become

$$
\begin{aligned}
&+\frac{q_o S c}{m V_o} C_{Y_\beta}\,\bar{v} - V_o \bar{r} + g\phi = 0 \\
&\frac{2}{b} C_{\ell_\beta}\,\bar{v} + C_{\ell_p}\,\bar{p} + C_{\ell_r}\,\bar{r} = 0 \\
&\frac{2}{b} C_{n_\beta}\,\bar{v} + C_{n_p}\,\bar{p} + C_{n_r}\,\bar{r} = 0 \\
&\dot{\bar{\phi}} = \bar{p}\,.
\end{aligned}
\tag{43}
$$

The C_{Y_β} term proved to have a negligible effect so it was also dropped as a matter of convenience. The characteristic root therefore satisfies the equation

$$
\begin{vmatrix}
0 & 0 & -V_o & g \\
\frac{2}{b} C_{\ell_\beta} & C_{\ell_p} & C_{\ell_r} & 0 \\
\frac{2}{b} C_{n_\beta} & C_{n_p} & C_{n_r} & 0 \\
0 & 1 & 0 & -\lambda
\end{vmatrix} = 0 \tag{44}
$$

Solving this equation for λ one gets for the time constant of decaying motion

$$
t_o = -\frac{1}{\lambda} = \frac{V_o}{g}\,\frac{C_{\ell_\beta} C_{n_p} - C_{\ell_p} C_{n_\beta}}{C_{\ell_\beta} C_{n_r} - C_{\ell_r} C_{n_\beta}}\,. \tag{45}
$$

If the sign of t_o should turn out to be negative the spiral would become tighter rather than decay. A criterion for spiral stability is therefore

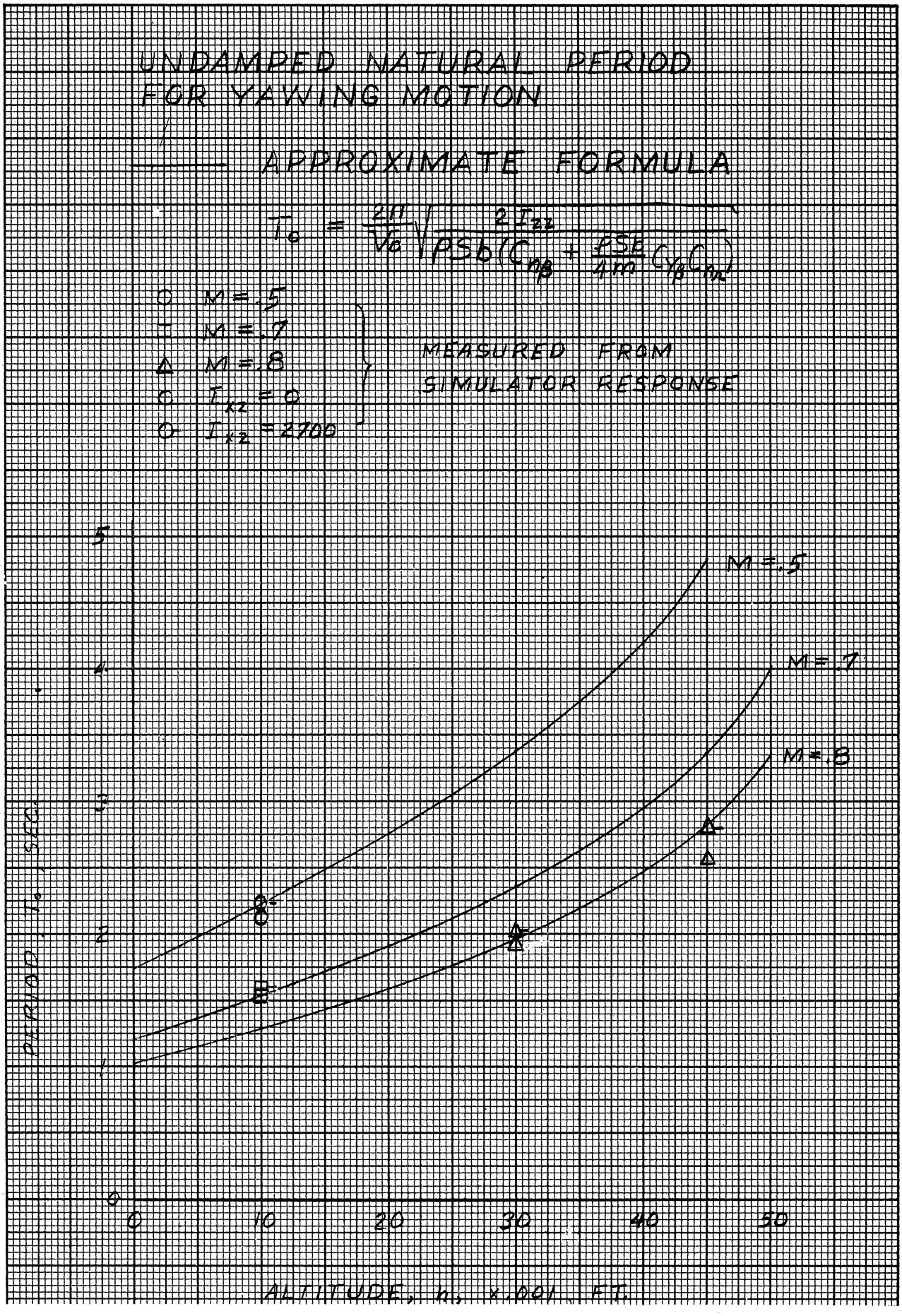

UNDAMPED NATURAL PERIOD FOR YAWING MOTION
APPROXIMATE FORMULA
$T_0 = \frac{2\pi}{V_0}\sqrt{\frac{2I_{zz}}{\rho S b\left(C_{n_\beta} + \frac{\rho S b}{4m} C_{Y_\beta} C_{n_{\dot{r}}}\right)}}$
MEASURED FROM SIMULATOR RESPONSE
M = .5
M = .7
M = .8
$I_{xz} = 0$
$I_{xz} = 2700$
PERIOD, T_0, SEC.
ALTITUDE, h, x.001 FT.
0
10
20
30
40
50
1
2
3
4
5

Figure 15

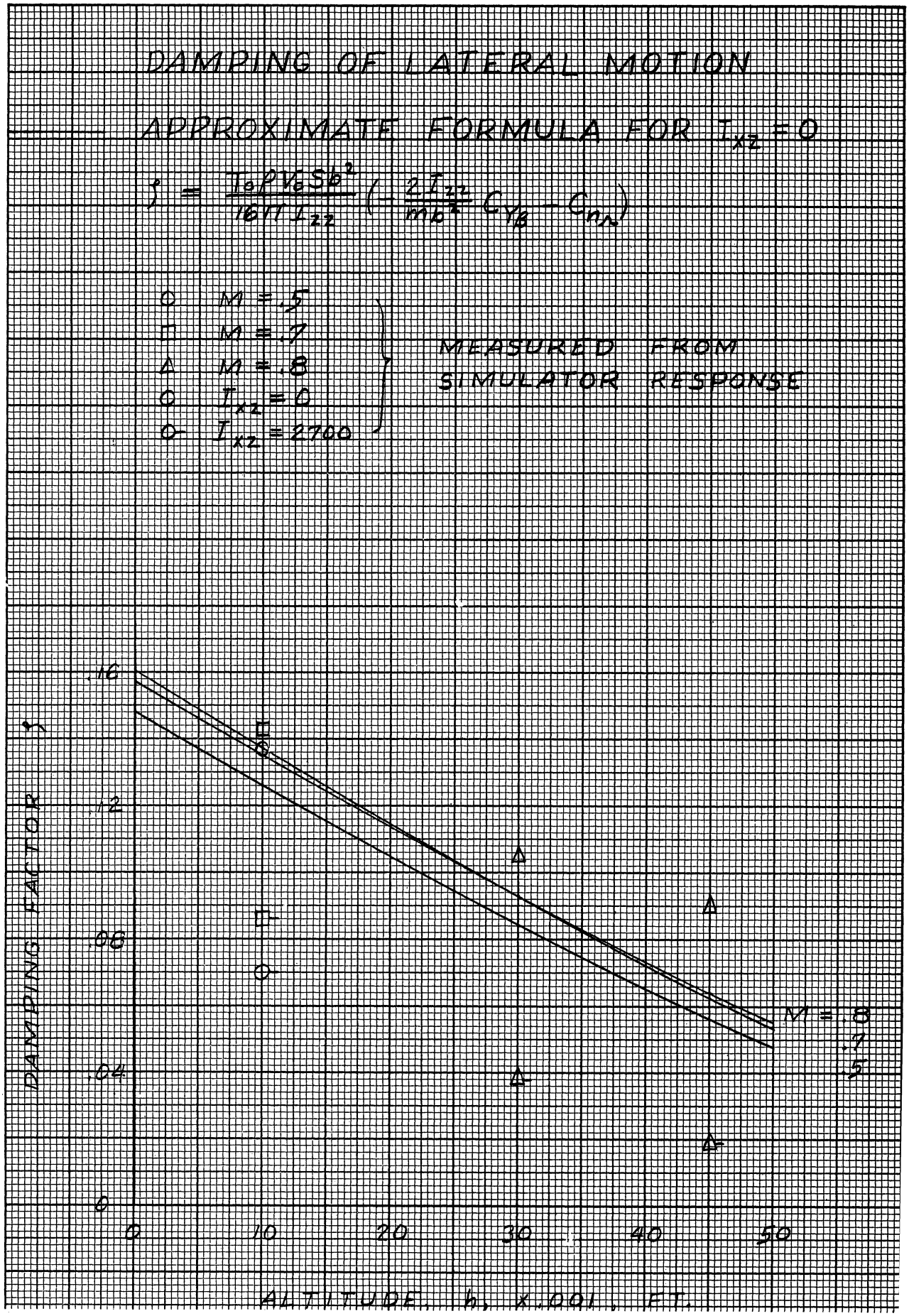

DAMPING OF LATERAL MOTION
APPROXIMATE FORMULA FOR $I_{xz} = 0$
$\zeta = \frac{T_0 \rho V_0 S b^2}{16 I_{zz}} \left(-\frac{2 I_{zz}}{m b^2} C_{Y_\beta} - C_{n_r} \right)$
○ $M = .5$
□ $M = .7$
△ $M = .8$
○ $I_{xz} = 0$
○ $I_{xz} = 2700$
MEASURED FROM SIMULATOR RESPONSE
DAMPING FACTOR ζ
.16
.12
.08
.04
0
0
10
20
30
40
50
ALTITUDE, h, X.001, FT.
M = .8
.7
.5

Figure 16

$$\frac{C_{\ell_\beta} C_{n_p} - C_{\ell_p} C_{n_\beta}}{C_{\ell_\beta} C_{n_r} - C_{\ell_r} C_{n_\beta}} > 0 . \qquad (46)$$

Formula (45) is compared with the simulator response in Figure 17. This motion is much slower than phugoid motion, yet the correlation is quite good.

When the simulator response to an initial value on $\bar{p}$ with $\bar{v}_i$, $\bar{r}_i$, and ϕ_i all zero is studied, it is found that the rolling velocity is rapidly damped and that very little oscillatory motion is excited, particularly at the lower altitudes. This can be seen in Figure 10. The effect of I_{xz} is not noticeable. This suggests that an approximate formula may be found by dropping all terms but $\bar{p}$ terms from the second of equations (35). The resulting equation is

$$\dot{\bar{p}} = \frac{\rho_o Sb^2}{2V_o I_{xx}} C_{\ell_p} \bar{p} \qquad (47)$$

The time constant of this motion is

$$t_o = -\frac{4I_{xx}}{\rho V_o Sb^2} \frac{1}{C_{\ell_p}} \qquad (48)$$

This is plotted in Figure 18. The time constant was calculated by measuring the time to damp to half-amplitude instead of measuring the decay over a longer period; this was done with the hope of minimizing the effect of the oscillating motion on the readings.

V. CORRELATION WITH FLIGHT TEST DATA

Figure 19 compares a simulator response trace with flight test data points for pitching motion. The initial conditions on the simulator variables were assumed to be zero for $\bar{\theta}$ and $\bar{u}$. Also $\bar{\alpha}_i = \alpha_o$, since for 2G acceleration the lift must be double the airplane weight, thus doubling the angle of attack. It was assumed that the pitching rate $\bar{q}_i$ corresponds to motion on a circle with radius such that the centripetal acceleration is one gravity; thus $\bar{q}_i = g/V_o$. The normal acceleration, according to equation (18), is $\dot{\bar{w}} - V_o \cos \alpha_o \bar{q}$. The simulator trace and the flight test points agree well with regard to shape although the simulator has a slightly longer period. The flight test points do not approach unity, which is abnormal.

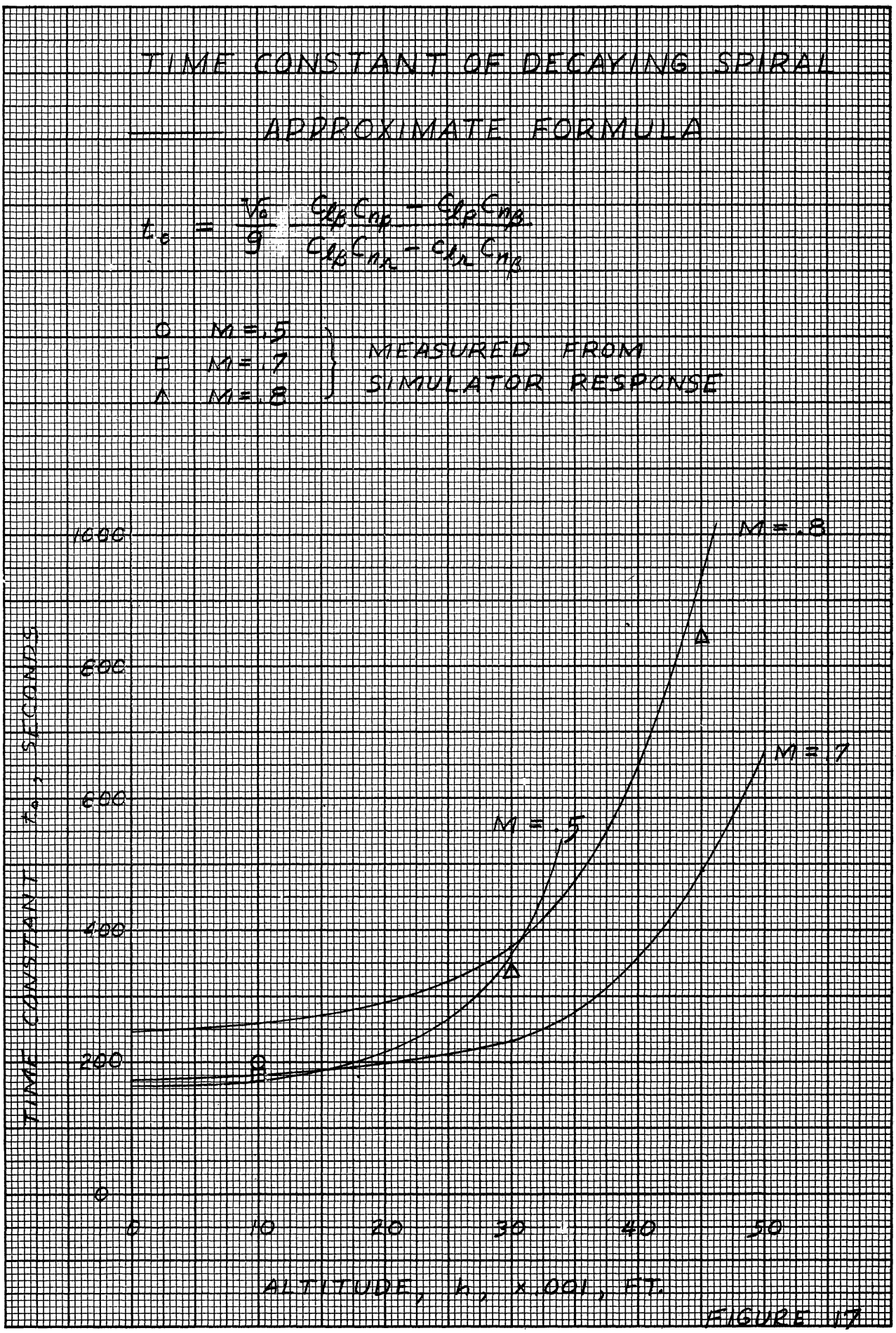

TIME CONSTANT OF DECAYING SPIRAL
APPROXIMATE FORMULA
$t_c = \frac{V_0}{g} \frac{C_{l_\beta} C_{n_p} - C_{l_p} C_{n_\beta}}{C_{l_\beta} C_{n_r} - C_{l_r} C_{n_\beta}}$
○ M = .5
□ M = .7
△ M = .8
} MEASURED FROM SIMULATOR RESPONSE
TIME CONSTANT, t_c, SECONDS
1000
800
600
400
200
0
0
10
20
30
40
50
M = .8
M = .7
M = .5
ALTITUDE, h, x .001, FT.
FIGURE 17

Figure 17

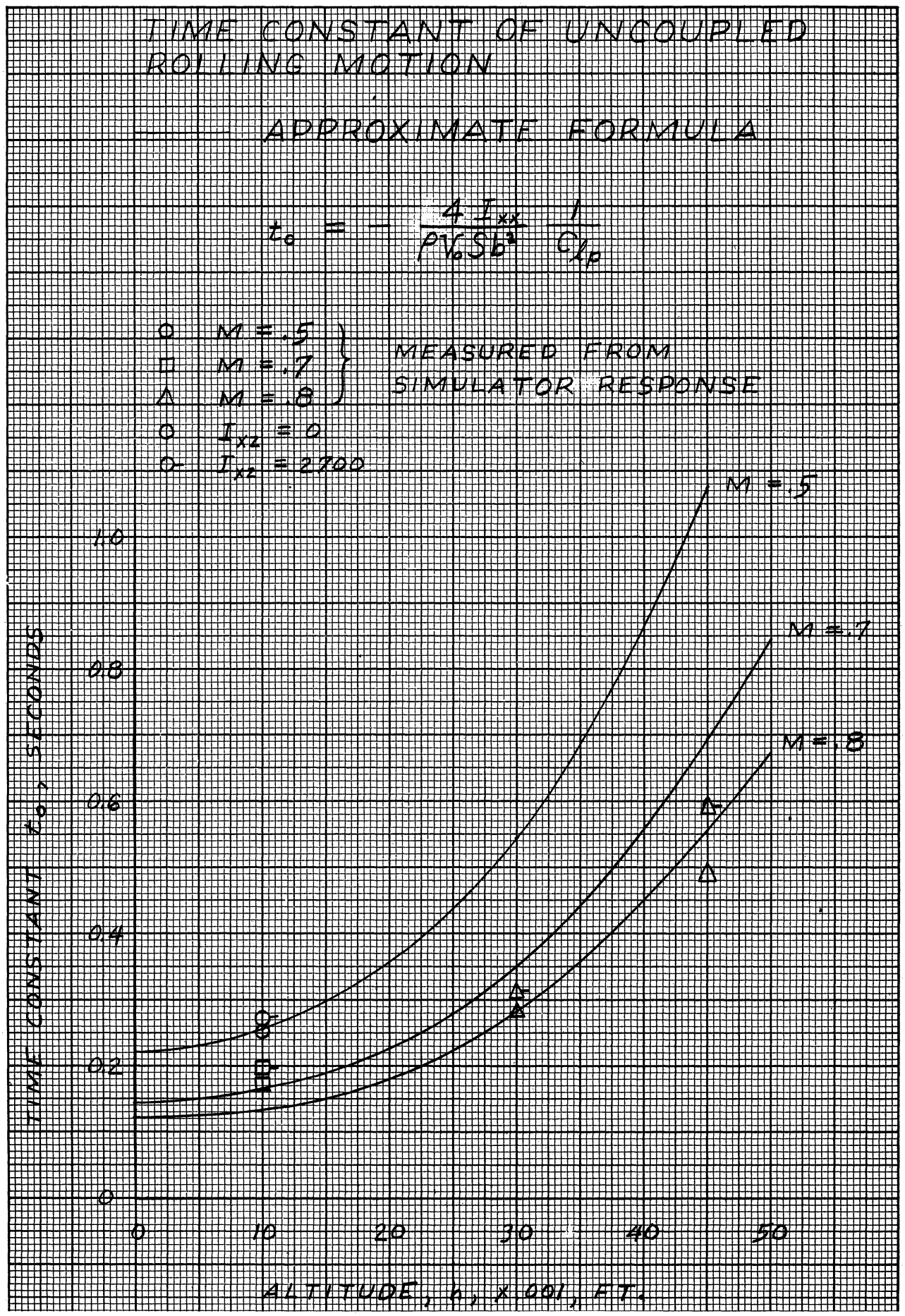

TIME CONSTANT OF UNCOUPLED ROLLING MOTION
APPROXIMATE FORMULA
$t_c = -\frac{4 I_{xx}}{\rho V_0 S b^2} \frac{1}{C_{l_p}}$
○ M = .5
□ M = .7
△ M = .8
MEASURED FROM SIMULATOR RESPONSE
○ I_{xz} = 0
○ I_{xz} = 2700
TIME CONSTANT, t_c, SECONDS
1.0
0.8
0.6
0.4
0.2
0
0
10
20
30
40
50
ALTITUDE, h, X 001, FT.
M = .5
M = .7
M = .8

Figure 18

NORMAL ACCELERATION, G'S
TIME SECONDS
FIGURE 16
FLIGHT TEST - SIMULATOR CORRELATION
MANEUVER: PULL UP TO 2G STABILIZED AND RELEASE
SIMULATOR RESPONSE
FLIGHT TEST NO 251-3

Figure 19

The angle of pitch necessary to have this effect in steady flight is 45 degrees which is much too high. There were no other measurements in this set of data which correspond to other variables computed by the simulator.

The lateral motion data shown in Figure 20 is more complete; it contains all four of the variables involved. No attempt was made to match the initial conditions of the flight test data but rather to obtain the best overall agreement through the first cycle taking all four traces into account. This seems to be the most reasonable approach since the test pilot is unable to center his controls instantly; this results in a distortion in the data during the first half second or so of motion. Many combinations of initial values were tried in an effort to get the best fit. Damping factor and period were measured from the simulator response and from each of the β, p, and r recordings of the flight test data with the results shown in the table.

Lateral motion M = .6 h = 40,000

Trace	Period	Damping Ratio
Simulator	2.75	.087
Flight-Test β	3.3	.17
Flight-Test r	3.1	.13
Flight-Test p	3.0	.14

The simulator, which is an almost ideal linear system, shows the same damping and period on all traces. The different values measured from the flight test data are an indication of nonlinearity or scatter in the data. The flight test points seem more reasonable if one follows the peak to peak values rather than zero to peak values. A variable zero error would explain many irregularities in the data. When the transient is finished the airplane appears to be left in a tighter spiral with more slip than the simulator. This is probably an indication of erroneous data since the airplane directional stability should reduce the sideslip nearly to zero in this case. It appears that the simulator roll rate is twice as great as the airplane roll rate. The apparent large discrepancy in the angle of bank probably is not important since a small amount of aileron control during this maneuver could make a big difference.

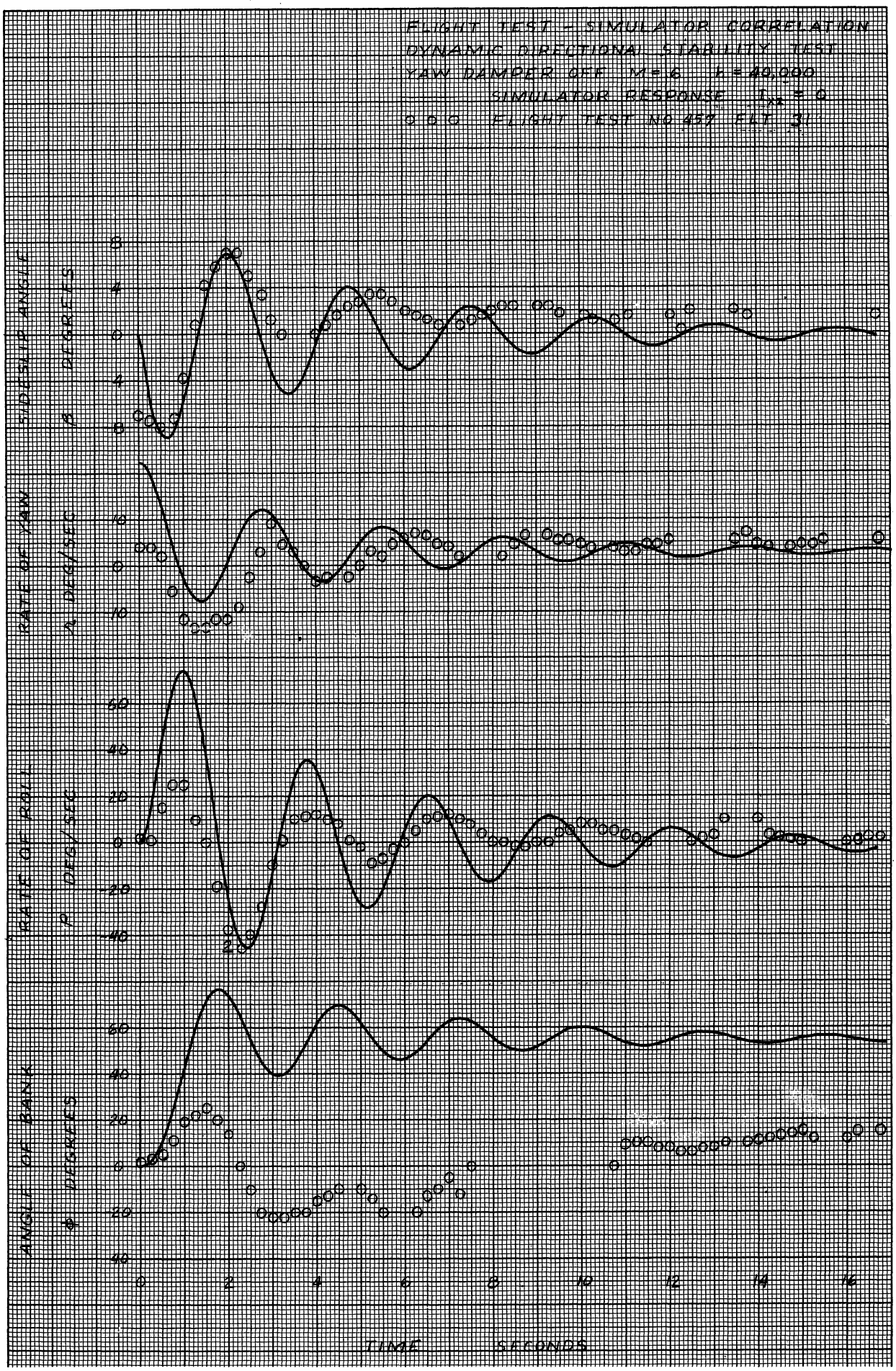

FLIGHT TEST - SIMULATOR CORRELATION
DYNAMIC DIRECTIONAL STABILITY TEST
YAW DAMPER OFF M=.6 h=40,000
SIMULATOR RESPONSE
FLIGHT TEST NO 457 FLT 31
SIDESLIP ANGLE
RATE OF YAW
RATE OF ROLL
ANGLE OF BANK
TIME SECONDS

Figure 20

This is because there are no large forces in the system which tend to reduce bank angle to zero.

More lateral motion data is shown in Figure 21. At this speed several trends seem to be reversed. The simulator damping is now too much rather than too little, and the simulator roll rate is half rather than double the airplane roll rate. The yaw-rate flight-test data is doubtless plotted 180 degrees out of phase. Since the slope of the sideslip angle is principally the negative of the yaw rate, the given flight-test data appears to be physically impossible. The simulator yaw rate is twice too large in this case. There was no angle of bank data available. Measurements from these traces are shown in the table below.

Lateral motion M = 0.8 h = 40,000 ft.

Trace	Period	Damping
Simulator	2.22	.093
Flight-Test β	2.53	.061
Flight-Test β	2.63	.093
Flight-Test p	2.50	.066

VI. MECHANIZATION OF THE EQUATIONS OF MOTION

Four speed-altitude cases were computed for both systems

$$\begin{aligned} M &= .5 & h &= 10,000 \\ M &= .7 & h &= 10,000 \\ M &= .8 & h &= 30,000 \\ M &= .8 & h &= 45,000 \end{aligned} \qquad (49)$$

The coefficients of equations (25) and (26) were evaluated using data from North American report NA-50-107A. The stability derivatives C_{m_q} and C_{L_q} vary with the position of the airplane center of gravity, which depends on the rockets and fuel carried. The cases considered were for no rockets and thirty percent of the fuel expended, which places the c.g. at the 24% point of the mean aerodynamic chord. The following physical constants of the F-86 were used:

S = 288 square feet

b = 37.1 feet

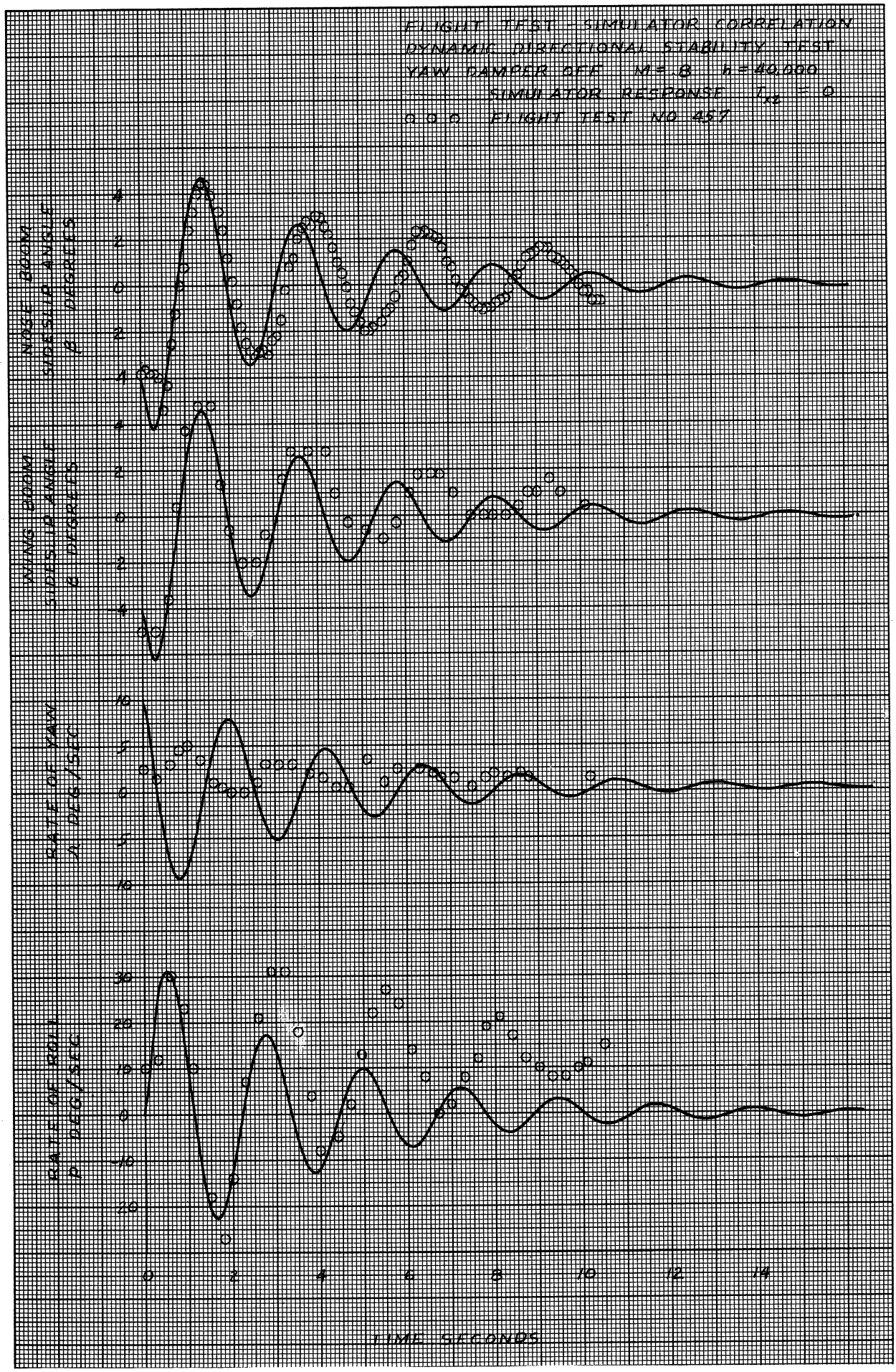

FLIGHT TEST - SIMULATOR CORRELATION
DYNAMIC DIRECTIONAL STABILITY TEST
YAW DAMPER OFF M = .8 h = 40,000
SIMULATOR RESPONSE I_{xz} = 0
FLIGHT TEST NO 457
SIDESLIP ANGLE DEGREES
ROLL RATE DEGREES/SEC
YAW RATE DEGREES/SEC
PITCH RATE DEGREES/SEC
TIME SECONDS

Figure 21

$$
\begin{aligned}
c &= 8.09 \text{ feet} \\
mg &= 15,500 \text{ pounds} \\
I_{xx} &= 8,625 \text{ slug feet squared} \\
I_{yy} &= 29,500 \quad " \quad " \quad " \\
I_{zz} &= 35,300 \quad " \quad " \quad " \\
I_{xz} &= 0 \text{ and } 2700 \quad " \quad " \quad "
\end{aligned}
\tag{50}
$$

The two values of I_{xz} were estimated to be the upper and lower limits. The equations for pitching motion derived from (30) are

$$
-\dot{\bar{u}} = +\underset{(1)}{\begin{Bmatrix} .008 \\ .012 \\ .006 \\ .003 \end{Bmatrix}} \bar{u} - \underset{(2)}{\begin{Bmatrix} .081 \\ .052 \\ .049 \\ .049 \end{Bmatrix}} \bar{w} + \underset{(3)}{\begin{Bmatrix} .296 \\ .194 \\ .325 \\ .648 \end{Bmatrix}} 100\,\bar{q} + .322\,\bar{\theta} \tag{4}
$$

$$
-\dot{\bar{w}} = +\underset{(5)}{\begin{Bmatrix} .059 \\ .042 \\ .040 \\ .041 \end{Bmatrix}} \bar{u} + 4\underset{(6)}{\begin{Bmatrix} .269 \\ .411 \\ .245 \\ .124 \end{Bmatrix}} \bar{w} - 10\underset{(7)}{\begin{Bmatrix} .533 \\ .746 \\ .790 \\ .772 \end{Bmatrix}} 100\,\bar{q} + \underset{(8)}{\begin{Bmatrix} .018 \\ .008 \\ .013 \\ .027 \end{Bmatrix}} \bar{\theta}
$$

$$
-100\,\dot{\bar{q}} = -\underset{(9)}{\begin{Bmatrix} .124 \\ .084 \\ .067 \\ .068 \end{Bmatrix}} \bar{u} + 4\underset{(10)}{\begin{Bmatrix} .539 \\ .768 \\ .398 \\ .202 \end{Bmatrix}} \bar{w} + 4\underset{(11)}{\begin{Bmatrix} .265 \\ .399 \\ .228 \\ .114 \end{Bmatrix}} 100\,\bar{q} \tag{51}
$$

$$
-100\,\dot{\bar{\theta}} = -100\,\bar{q}
$$

Each set of four numbers corresponds to each of the four speed-altitude cases (49). The equations for lateral motion derived from (31) are

$$
-\dot{\bar{v}} = \underset{(1)}{\begin{Bmatrix} .221 \\ .325 \\ .175 \\ .086 \end{Bmatrix}} \bar{v} - \underset{(2)}{\begin{Bmatrix} .301 \\ .197 \\ .327 \\ .652 \end{Bmatrix}} 100\,\bar{p} + 10\underset{(3)}{\begin{Bmatrix} .540 \\ .757 \\ .798 \\ .778 \end{Bmatrix}} 100\,\bar{r} - \underset{(4)}{.322\,(100\,\bar{\phi})}
$$

$$-100\dot{\bar{p}} + \begin{pmatrix}0\\31.3\end{pmatrix}\dot{\bar{r}} = 10\begin{Bmatrix}.540\\.681\\.441\\.267\end{Bmatrix}\bar{v} + 10\begin{Bmatrix}.400\\.611\\.360\\.184\end{Bmatrix}100\,\bar{p} - 4\begin{Bmatrix}.297\\.385\\.268\\.157\end{Bmatrix}100\,\bar{r} \qquad (52)$$

(5) (6) (7)

$$-100\dot{\bar{r}} + \begin{pmatrix}0\\7.65\end{pmatrix}\dot{\bar{p}} = -4\begin{Bmatrix}.357\\.527\\.302\\.145\end{Bmatrix}\bar{v} + \begin{Bmatrix}.067\\.018\\.039\\.054\end{Bmatrix}100\,\bar{p} + \begin{Bmatrix}.476\\.778\\.405\\.186\end{Bmatrix}100\,\bar{r}$$

(8) (9) (10)

$$-100\dot{\bar{\phi}} = -100\,\bar{p} - \begin{Bmatrix}.056\\.026\\.041\\.084\end{Bmatrix}\bar{r}$$

(11)

The computer circuit diagrams for solving these equations are shown in Figures 22 and 23. The conventional symbols used there are as follows: A triangle indicates a high gain inverting DC amplifier with a one megohm feedback resistor; in this case the amplifier serves as a sign-changing summer. A triangle with a double vertical bar indicates the feedback element is a one microfarad capacitor; thus the amplifier acts as a sign-changing integrator-summer. The input resistors are one megohm unless the numbers 4 or 10 are shown, in which case the resistor is 1/4 or 1/10 megohm. A circle with a number indicates a potentiometer which multiplies the voltage according to the coefficients of equations (51) and (52), identified by the circled numbers. All the circuit connections are not indicated in order that the diagram may be simplified. When two or more points are labeled by the same variable a common connection is implied.

In the case of lateral motion two values of I_{xz} were used. When $I_{xz} = 0$ the problem is straightforward because the equations (31) are solved explicitly for $\dot{\bar{p}}$ and $\dot{\bar{r}}$. When $I_{xz} = 2700$ equations (31) are solved for p' and r' where

$$\bar{p}' = \bar{p} - .313\,\bar{r}$$
$$\bar{r}' = \bar{r} - .0765\,\bar{p}. \qquad (53)$$

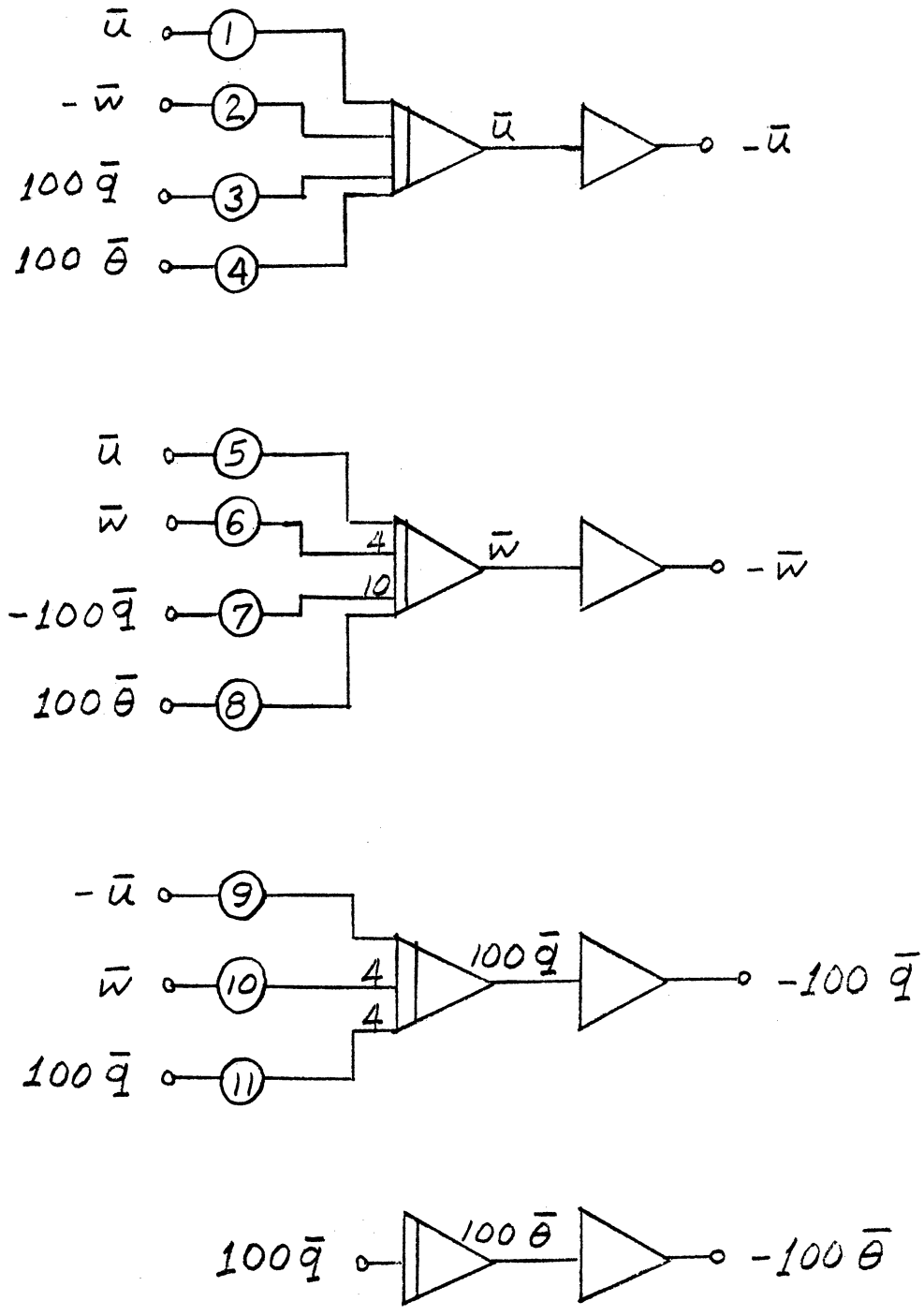


Figure 22. Computer Circuit for Pitching Motion.

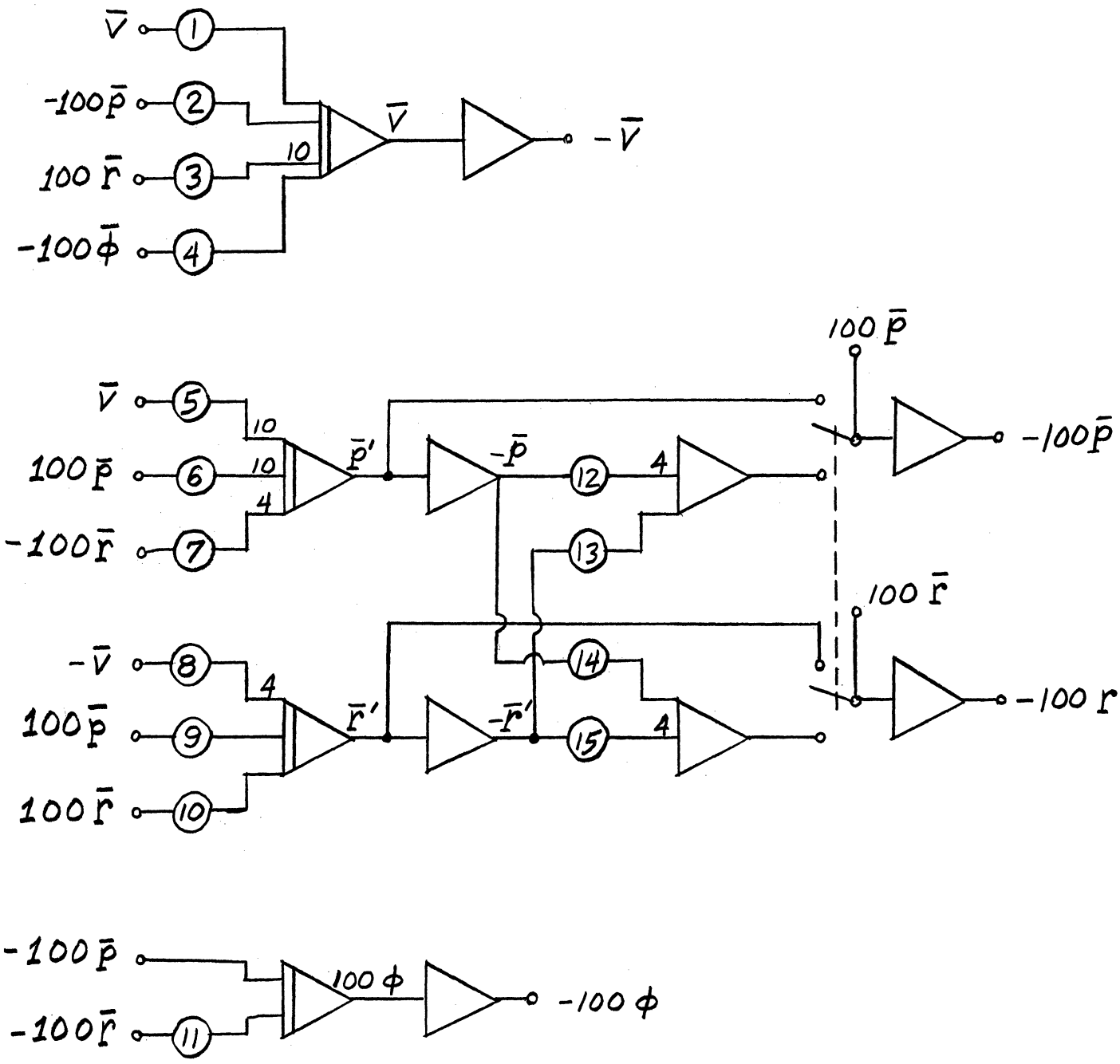


Figure 23. Computer Circuit for Lateral Motion.
Switch up for $I_{xz} = 0$.
Switch down for $I_{xz} = 2700$.

Equations (53) are solved for $\bar{p}$ and $\bar{r}$ with the result

$$\left.\begin{aligned} p &= \underset{(12)}{4 \times .256}\ \bar{p}' + \underset{(13)}{.320}\ \bar{r}' \\ \bar{r} &= \underset{(14)}{.078}\ \bar{p}' + \underset{(15)}{4 \times .256}\ \bar{r}' \end{aligned}\right\} \qquad (54)$$

The circuit for computing lateral motion (Figure 23) was designed so that either value of I_{xz} could be chosen by throwing one switch.

UNIVERSITY OF MICHIGAN
3 9015 03483 3502